SEMMELWEIS EGYETEM

DOKTORI ISKOLA

Ph.D. értekezések

3348.

GREBUR KINGA

Szív- és érrendszeri betegségek élettana és klinikuma

című program

Programvezető: Dr. Merkely Béla, egyetemi tanár

Témavezető: Dr. Szűcs Andrea, egyetemi docens

The imaging, genetic and clinical characteristics of left ventricular hypertrabeculation

PhD thesis

Kinga Grebur

Semmelweis University Doctoral School

Cardiovascular Medicine and Research Division

Supervisor: Andrea Szűcs, MD, Ph.D

Official reviewers: Annamária Kosztin MD, Ph.D
Gergely Ágoston MD, Ph.D

Head of the Complex Examination Committee: Alán Alpár MD Ph.D

Members of the Complex Examination Committee: László Cervenák MD Ph.D
Miklós Tóth MD Ph.D

Budapest
2025

Table of Contents

List of Abbreviations

ACM = arrhythmogenic cardiomyopathy

ACMG = American College of Medical Genetics and Genomics

AVNRT = atrioventricular nodal reentry tachycardia

B = benign

bSSFP = balanced steady-state free precession

C = control group

CC = conventional contouring post-processing method

CCW = counterclockwise

CI = confidence interval

CL= compact layer

CLT=compact layer thickness

CMP = cardiomyopathy

CMR = cardiac magnetic resonance imaging

CMR-FT = cardiac magnetic resonance imaging feature-tracking method

CRT-D = cardiac resynchronization therapy with defibrillator

CW = clockwise

DCM = dilated cardiomyopathy

DSP = desmoplakin

ECG = electrocardiogram

Echo-ST = echocardiography speckle-tracking method

EDVi = end-diastolic volume index

EF = ejection fraction

ESVi = end-systolic volume index

GCS = global circumferential strain

GLS = global longitudinal strain

HCM = hypertrophic cardiomyopathy

HF = heart failure

HFmrEF = heart failure with mid-range ejection fraction

HFrEF = heart failure with reduced ejection fraction

HR = hazard ratio

ICC = intraclass correlation coefficient

ICD = implanted cardiodefibrillator

LBBB = left bundle branch block

LGE = late gadolinium enhancement

LP = likely pathogenic

LV = left ventricle

LVEF = left ventricular ejection fraction

LVNC = left ventricular noncompaction

NCBI = National Center for Biotechnology Information

NGS = next-generation sequencing

OMIM = Online Mendelian Inheritance in Man

P = pathogenic

QTc = corrected QT interval

RBR = rigid body rotation

RV = right ventricle

SA = short axis view

SCD = sudden cardiac death

SD = standard deviation

SVi = stroke volume index

TB = threshold-based post-processing method

TL=trabecular layer

TMi = total muscle mass index

TPMi = trabeculated and papillary muscle mass index

VUS = variant of uncertain significance

1. Introduction

1.1 Ventricular trabeculation and hypertrabeculation

1.1.1 Embryogenesis and the role of trabeculae

In healthy individuals, the myocardium is formed by a subepicardial compact layer (CL) and a thin subendocardial noncompact or trabecular layer (TL). This trabecular meshwork is more pronounced in the apex, especially in the anterior and lateral apical segments (1).

Trabeculae have a special role in maintaining the mechanical and electrical function of the heart; moreover, trabecular complexity is proportional to the cardiac contractile capacity, which influences the ejection fraction (2). Cardiac models emphasize the importance of optimal trabeculation, as the appropriate quantity reduces left ventricular (LV) stress (3). However, hypertrabeculation might result in LV dilatation, decreased cardiac function, and interestingly in ventricular conduction disturbances through the poor development of the Purkinje fibers (3, 4).

In the literature, several theories exist regarding the embryological development of the trabecular and compact myocardium, with the current consensus supporting the independence of the CL and TL. Until recently, the trabecularization-compaction theory was thought to occur in the early embryological period (5, 6) by forming hypertrabeculation if compaction is not achieved (6). According to the novel theory, the TL and CL develop independently with a decreasing noncompact/compact ratio over time (7, 8). This independent development is supported by studies proving the normal evolution of the CL even after inhibition or stimulation of the TL (4, 9). Another new finding is discovering a middle hybrid myocardial zone between the compact and noncompact regions (9).

1.1.2 The spectrum of trabeculation

The spectrum of normal trabeculation is wide, and despite the proposed reference ranges, the border between normal and excessive trabeculation is still not well defined (1, 10-12).

Based on the literature, the trabecular meshwork has an individual pattern, and similarly to other biometric parameters, the trabeculated and papillary mass (TPMi) and the thickness of the TL could vary on sex and race as a more expressed trabeculation could appear in males and individuals from African and Afro-American races (12, 13).

Moreover, trabeculation might have a dynamic characteristic in the same individual, such as described by Bentatou et al. TPMi decreases with age and increasing stroke volume (SVi) (1, 12, 14, 15).

This vulnerable issue of normal and excessive trabeculation has become the subject of renewed interest in the recent period due to the 2023 European Society of Cardiology (ESC) Guidelines for the Management of Cardiomyopathies (CPM) and the State of the art review by Petersen et al. (10, 16). According to these recommendations, hypertrabeculation or excessive trabeculation terminology is preferred over the previously used noncompaction.

Large studies in the literature report the estimated prevalence of hypertrabeculation between 0.02 and 0.14% (6, 10), whereas the prevalence of an increased TL/CL ratio could be even higher in the healthy population (11, 17, 18). However, it should be emphasized that this hypertrabeculated morphology was not associated with increased mortality in otherwise healthy individuals, and according to Petersen et al., after careful examination, it could be considered a normal variant in healthy individuals (10, 17).

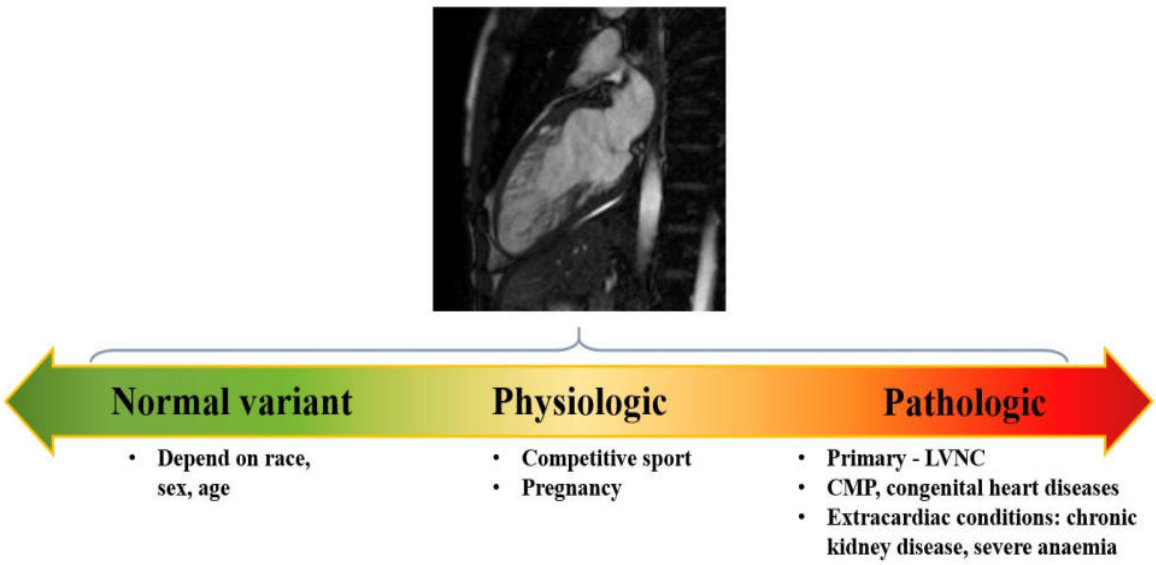

Figure 1: The spectrum of hypertrabeculation ranging from asymptomatic, healthy individuals, through physiological hypertrabeculation to pathological forms. *LVNC = left ventricular noncompaction, CMP = cardiomyopathy. Image belongs to the Semmelweis University, Heart and Vascular Center.*

1.1.3 Physiological hypertrabeculation

The mechanism of physiological hypertrabeculation is characterised by functional changes, such as increased preload, that trigger structural remodeling. Whereas the proliferative capacity of cardiomyocytes is limited in adults, the remodeling process is mainly manifested by the hypertrophy of the pre-existing trabeculae (19). This process provides faster and greater diastolic filling, higher cardiac output, better oxygenation, and longer duration of muscle activity (19).

One of the most commonly known forms of transient physiological hypertrabeculation was described in elite athletes (sports activity >10 hours per week) as part of the cardiac adaptation to increased SV, a phenomenon known as „the athlete's heart" (20).

A study of Olympic athletes described the prevalence of excessive trabeculated phenotype up to 18% with significant gender differences: nearly 50% of men and only 4% of women showed increased grey zone TL (19-22). Interestingly, it has a dynamic pattern, becoming more prominent in the most intense training periods (21). On the contrary, following the cessation of competitive sport, volumes normalize, and rapid reverse remodeling leads to the restoration of normal trabeculation (23, 24).

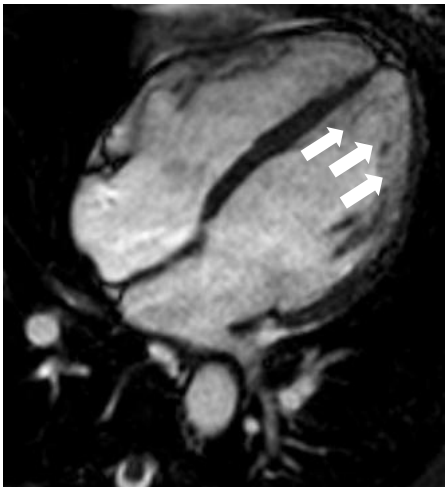

Figure 2: Physiologic hypertrabeculation of a competitive athlete on long-axis four-chamber CMR image. *White arrows show the apical trabecular meshwork. CMR = cardiac magnetic resonance imaging. The image belongs to the Semmelweis University, Heart and Vascular Center.*

Regarding the differential diagnostic aspect of cardiac adaptation, cardiac magnetic resonance imaging (CMR), Holter monitoring, and exercise echocardiography could help to distinguish between physiological hypertrabeculation induced by sports activity and its pathological form (20, 22). As indicated in the ESC Guideline on sports cardiology, the suspicion of pathology should arise only if decreased cardiac function (LV ejection fraction - LVEF<50%), symptoms, or a positive family history of noncompaction are present (20). It is important to note that no major cardiovascular events were reported in excessive trabeculated athletes without LV dysfunction, therefore, no restriction is advised for elite athletes with incidentally discovered hypertrabeculation and otherwise negative cardiac findings (25).

Another form of transient physiologic hypertrabeculation could occur during pregnancy. According to Gati et al., a significant increase in trabeculation was described in one-quarter of the studied healthy women, and 10-20% of them reached the criteria of noncompaction at the end of pregnancy (15). This excessive trabeculated morphology regressed quickly after birth and disappeared completely in 73% of cases over the two-year follow-up period (15).

1.1.4 Pathological hypertrabeculation

Regarding pathological hypertrabeculation, the primary, isolated hypertrabeculation or so-called LV noncompaction (LVNC) and the secondary excessive trabeculated phenotype should be distinguished. More information about LVNC is provided under the 1.1.5 subheading.

In the secondary form, hypertrabeculation is present along with a previously associated cardiac or extracardiac (e.g. renal and hematological diseases) condition.

The cardiac etiology of excessive trabeculation in congenital heart diseases, most frequently present in Ebstein anomaly, has two defining factors: genetic mutations and hemodynamic changes that influence together the myocardial development (26, 27).

Similarly, a hypertrabeculated phenotype could be observed in some types of genetically determined CMP, especially in dilated (DCM), arrhythmogenic (ACM), and hypertrophic (HCM) forms (28).

DCM is defined by LV dilation and systolic dysfunction in the absence of ischemic or other causes (16). With a prevalence of 0.036-0.400 % in the adult population, DCM is the most common cause of heart failure (HF) and cardiac transplantation in adults (16).

The diagnosis of ACM is based on the revised Task Force criteria, including right ventricular (RV) dilation and dysfunction, histological involvement, and electrocardiography (ECG) abnormalities (16, 29). The prevalence of ACM is 0.078% in adults and is characterized by malignant ventricular arrhythmias and HF (16).

The prevalence of HCM is around 0.2 % in the adult population, and the condition is characterized by abnormal thickening of the LV wall, which could not be explained by mechanical factors (16). This morphology leads to symptoms such as shortness of breath, arrhythmias, and angina and increases the risk of sudden cardiac death (SCD) (16).

These last two CMPs are the most common cause of SCD in young athletes (30, 31).

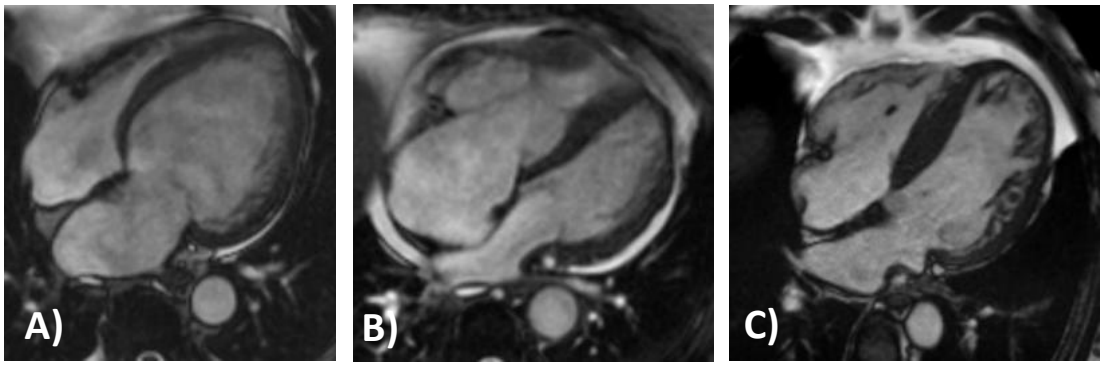

Figure 3: Different forms of secunder hypertrabeculation on long-axis four-chamber CMR images*. Image (A) presents dilated cardiomyopathy with dilated left ventricular cavity and thinned wall; image (B) describes arrhythmogenic cardiomyopathy with dilated, fatty infiltrated right ventricle; and image (C) shows hypertrophic cardiomyopathy with thickened left ventricular wall. CMR = cardiac magnetic resonance imaging. Images belong to the Semmelweis University, Heart and Vascular Center.*

As hypertrabeculation is a secondary finding in these abovementioned CMPs, the novel guidelines recommend that patients should be managed based on the underlying primary CMP and cardiac symptoms (10). However, the hypertrabeculated phenotype has relevance in differential diagnosis, especially in infants and children with primary LVNC

as they should be screened for neuromuscular, other genetic or metabolic diseases (10, 16).

1.1.5 Left ventricular noncompaction

In primer, persistent, isolated left ventricular hypertrabeculation the myocardium is formed by a thin CL and a thickened TL with spongy myocardial network and deep intertrabecular recesses. In order to differentiate this condition from normal hypertrabeculation, in the present work, we continue to refer to it as excessive trabeculation or LVNC.

The prevalence of LVNC is not well defined because of its varied morphology and clinical presentation. However, it is estimated to be a rare condition in about 0.014% to 0.26% of cases, with the incidence being two to three times higher in men (32). A higher occurrence was described in children and individuals with a positive family history, as ¼ - ½ of LVNC patients have LVNC, DCM, ACM, or HCM among the family members (33-35).

Regarding the etiology of LVNC, embryological studies and family accumulation highlight the role of genetic mutations in the development of trabecular meshwork (7, 10). The heritability of LVNC is estimated at about 20%, although genetic mutations were present in half of end-stage HF or children LVNC study populations (35, 36). Until recently, up to 40 different gene loci were identified in relation to hypertrabeculation, coding sarcomeric, cytoskeletal, mitochondrial, desmosomal, and ion channel proteins (10, 34, 37). According to these studies, the most common mutations affect TTN, TNNT2, MYH7, MYBPC3, and ACTC1 (10, 38, 39). Genetic mutations frequently overlap with other CMP and myocardial diseases; however, truncating variants in MYH7, ACTN2, and PRDM16 are thought to be specific for hypertrabeculation (10).

The morphological diagnosis of LVNC is based on CMR and echocardiography examinations; the current diagnostic criteria are presented in subsections 1.2.1 and 1.2.2.

When analysing the clinical presentation of LVNC, a wide spectrum of hypertrabeculation ranging from the asymptomatic morphological variant mentioned above (subsection 1.1.2) to end-stage HF should be considered (10, 16). The spectrum of cardiac symptoms is also diverse, such as palpitations, syncope, dyspnoe, atypical chest

pain could all manifest in LVNC patients. In terms of cardiovascular complications, there are three hallmarks of LVNC: LV systolic dysfunction, thromboembolic events, and ventricular arrhythmias (16). Although no precise connection was described between the extent of trabecular meshwork and LV function, a decrease in LVEF could occur in LVNC, especially in patients carrying multiple genetic mutations (37). Van Waning et al. noted HF as the most common complication of LVNC, being present or occurring during the follow-up in 44% of their children and 58% of their adult LVNC population (37). In our working group, the LVEF decreased by 10% over a 10-year follow-up in 5-10% of our LVNC cohort, and according to the Hungarian database, the LVNC accounted for 2% of the indications for heart transplantation. Additionally, literature data associate genotype-positive status with an increased incidence of end-stage heart failure, heart transplantation or death. (34, 40).

Thromboembolic events in LVNC have been described with variable incidence ranging from 0 to 38%, occurring mainly in adults rather than in the pediatric LVNC population (41). In sinus rhythm, the prevalence of systemic embolism, such as juvenile stroke, was most closely related to LV systolic dysfunction (41).

According to van Waning, arrhythmias represented the second most frequent symptom, with a prevalence of 26% at initial presentation (37). Malignant ventricular arrhythmias such as ventricular tachycardia and fibrillation were linked to certain genetic mutations, e.g., DSP, suggesting the existence of an arrhythmogenic LVNC phenotype (34). In addition, supraventricular arrhythmias and ECG abnormalities, e.g., intraventricular conduction delay, Wolf-Parkinson-White syndrome, repolarisation abnormalities, and prolonged QTc were also reported in LVNC patients (42).

Regarding the clinical management of LVNC, the novel Petersen statement recommends the symptom-based approach rather than the phenotype-based one (10). Therefore, major cardiovascular complications such as HF, thromboembolic events, and arrhythmias should be treated according to the current national and international guidelines (10, 16).

The importance of risk stratification in LVNC individuals must be emphasized because of the various clinical manifestations. Although no precise protocol exists, several parameters have been identified as indicators of complications and major cardiovascular events. Among them, an increased left ventricular end-diastolic volume index (LVEDVi)

with a hazard ratio (HR) of 3.65 (p = 0.002), the presence of late gadolinium enhancement (LGE) with an HR of 4.382 (p < 0.001) and decreased LVEF with an HR of 3.115 (p=0.019) were the most significant (43).

Thus, individuals with LVNC morphology on CMR or echocardiography should be screened for a family history of CMP or SCD, personal medical history, abnormalities on ECG and Holter monitors, LGE on CMR images, and genetic mutations (10, 43, 44). More information about the indication for genetic testing is presented in subsection 1.2.4.

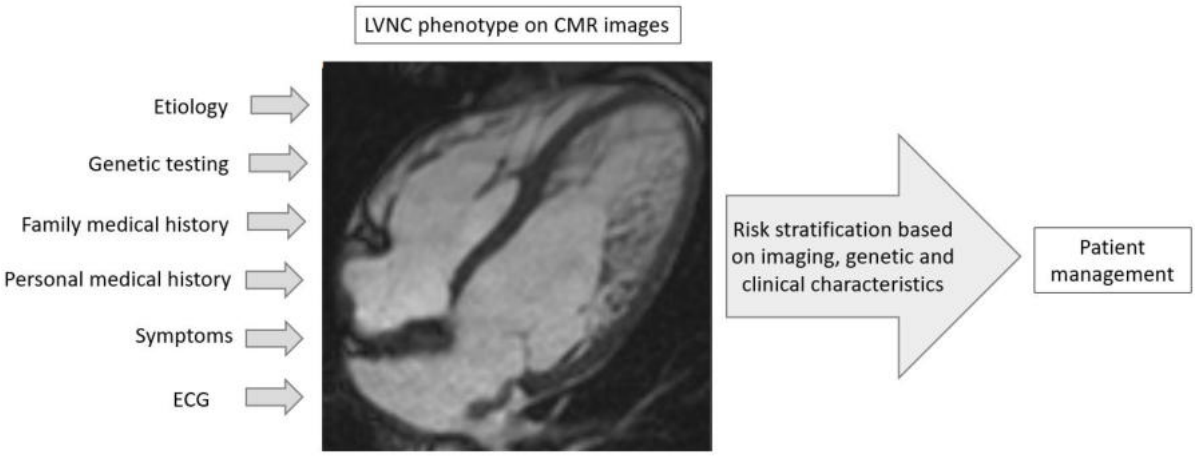

Figure 4: Risk stratification algorithm of left ventricular noncompaction phenotype individuals. *LVNC = left ventricular noncompaction, CMR = cardiac magnetic resonance imaging, ECG = electrocardiogram. Image shows the hypertrabeculation on a long-axis four-chamber CMR scan. Image was partially published in (45).*

As a result of risk stratification, individuals with LVNC morphology and clinical manifestations are noted for follow-up, whereas those with LVNC phenotype without symptoms, positive family and personal medical history, and otherwise normal imaging and ECG findings should not undergo further investigations (10).

1.2 Diagnostic tools in hypertrabeculation

The diagnosis of LVNC should be approached from three directions: (1) analyzing the hypertrabeculated phenotype on echocardiography and/or CMR images, (2) investigating the etiology and the presence of genetic mutations, and (3) evaluating the clinical manifestation through cardiac symptoms, family and personal medical history, ECG and if necessary additional examinations.

1.2.1 The role of echocardiography in the diagnosis of left ventricular noncompaction

The first in vivo descriptions of LVNC were reported by using transthoracic echocardiography, and to date, this modality remains the first-line imaging tool in everyday clinical practice (46). Due to its wide availability, echocardiography is used not only in the screening of suspected individuals and family members of LVNC patients but also in the follow-up of diagnosed LVNC individuals (43).

Several echocardiography criteria have been reported for the quantitative description of LVNC, which quantify the thickness of CL and TL, e.g., the Chin, Jenni, and Stöllberger criteria (46-48). Of these, clinicians most commonly use the Jenni criteria, which define a TL/CL>2 ratio on parasternal short-axis (SA) end-systolic images in the absence of a coexisting structural disease and perfusion in intertrabecular recesses on color Doppler images (47). Another aspect of the Jenni criteria is the presence of the deep intertrabecular recesses examined with the color Doppler echocardiography alongside the excessive trabeculated myocardium (47).

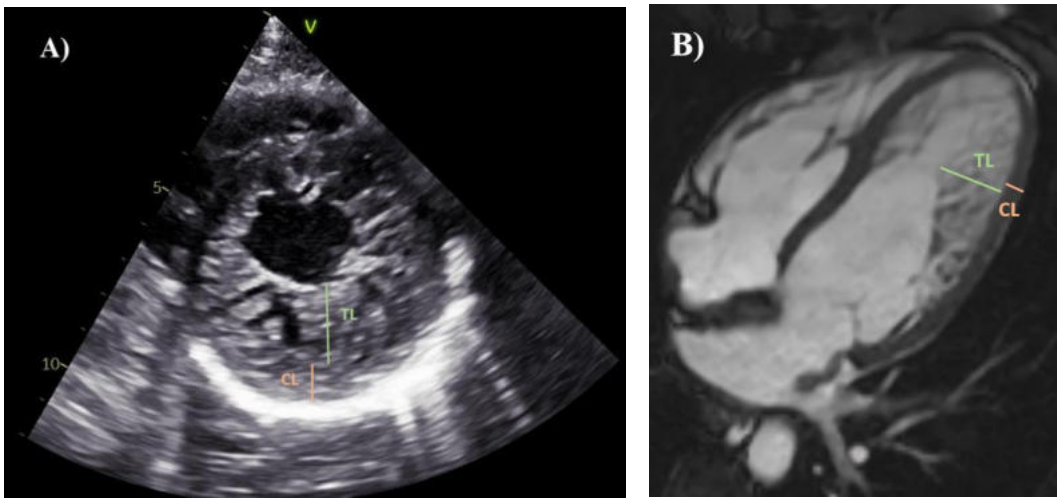

Figure 5: Imaging diagnostic criteria of left ventricular noncompaction. *The echocardiographic image (A) describes the Jenni criteria on a parasternal short-axis end-systolic frame. The CMR image (B) represents the Petersen criteria on a four-chamber long-axis end-diastolic scan. CL = compact layer (red line), TL = trabeculated layer (green line), CMR = cardiac magnetic resonance imaging. Images belong to the Semmelweis University, Heart and Vascular Center.*

Additionally, to differentiate the hypertrabeculated phenotype from false tendons, muscular bands, apical thrombus or cardiac tumors, transesophageal or 3D echocardiography and the application of a contrast agent or a CMR examination could be necessary (43, 44, 49).

1.2.2 The role of cardiac magnetic resonance imaging in the diagnosis of left ventricular noncompaction

Due to the technical developments in CMR imaging, new directions and increasing interest in LV hypertrabeculation have emerged in recent decades (1, 2, 10, 50, 51).

CMR is considered the gold standard diagnostic tool in LVNC and is usually performed to confirm the diagnosis raised by echocardiography, although occasionally provides the incidental, first description of excessive trabeculation (10, 43). All LVNC diagnostic criteria using CMR aim to capture the amount of trabeculation in terms of mass, volume, thickness, or fractal; the most well-known criteria of them were reported by Petersen, Jacquier, Grothoff, Stacey and Captur (10, 50, 52-54). Although concerns were raised in the literature due to the small study population of Petersen et al., the TL/CL>2.3 Petersen criteria is still widely used (10, 16). The criteria described by Jacquier et al. could be used additionally to identify LVNC when the LVTPMi represents >20% of the LVTMi (52).

A more detailed, objective analysis of the trabecular meshwork is provided by the threshold-based (TB) post-processing CMR analyzing method, which is highly reproducible and has good inter- and intraobserver variability (55-57). In contrast to the conventional contouring technique (CC), which considers the intracavitary myocardium as part of the blood volume, the TB method detects the different signal intensities of blood and myocardium so it is able to distinguish TPMi from the blood volume (56-58). Although Jaspers et al. validated the TB method at a 70% threshold, in the scientific literature and clinical practice, the default setting of 50% is preferred (12, 56, 57, 59).

Beyond the analysis of morphology and functional parameters on CMR images, the use of gadolinium-based contrast agent could provide additional information as late gadolinium enhancement (LGE) was identified as a predictor of poor outcome in LVNC, especially in the cases with genetic involvement (60-62).

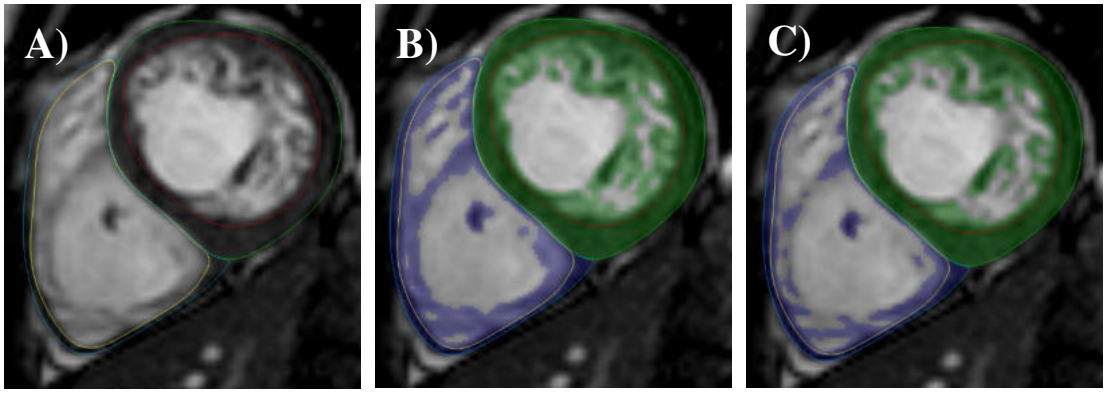

Figure 6: The conventional countouring (image A) and threshold-based post-processing methods with 70% (image B) and 50% (image C) thresholds on short-axis CMR images of left ventricular noncompaction *(63).* *According to the conventinal countouging technique (image A), myocardial mass is defined as the area between the endocardial contour (red for LV and yellow for RV) and epicardial contour (green for LV and blue for RV), while the area within the endocardial border is considered as blood volume. In contrast, the threshold-based method (images B and C) visualizes the intracavitar trabecular meshwork by highlighting it in green (LV) and purple (RV). Consequently, the area between the endocardial and epicardial borders corresponds to the compact myocardium. LV = left ventricle, RV = right ventricle, CMR = cardiac magnetic resonance imaging.*

1.2.3 Cardiac deformation analysis

Further evaluation of the cardiac function is possible with deformation analysis by using the echocardiography speckle-tracking (Echo-ST) and CMR feature-tracking (CMR-FT) post-processing methods.

Myocardial strain measures the percentage difference of the contracted and relaxed length of myocardial fibers by tracking the intramyocardial speckles with Echo-ST and the endocardial border with CMR-FT through the cardiac cycle (64, 65). Thus, a reduction in the global longitudinal (GLS) and circumferential (GCS) strains could be an important marker of subtle mechanical changes, especially in LVNC with preserved LVEF and yet impaired function (66, 67). Interestingly, apical circumferential strain impairment was a hallmark of LVNC patients with HF compared to DCM (68).

Another cardiac deformation parameter is cardiac rotation. The clockwise (CW) basal and counterclockwise (CCW) apical end-systolic rotation in healthy, mature myocardium

is responsible for the suction effect of LV and, thus, normal cardiac function (65, 69, 70). In the literature, four types of cardiac rotational patterns were described: the abovementioned (1) normal rotation; (2) reverse rotation, which is the opposite of normal; (3) positive rigid body rotation (RBR) with positive (CCW) apical and basal rotation; and (4) negative RBR with negative (CW) apical and basal rotation (65).

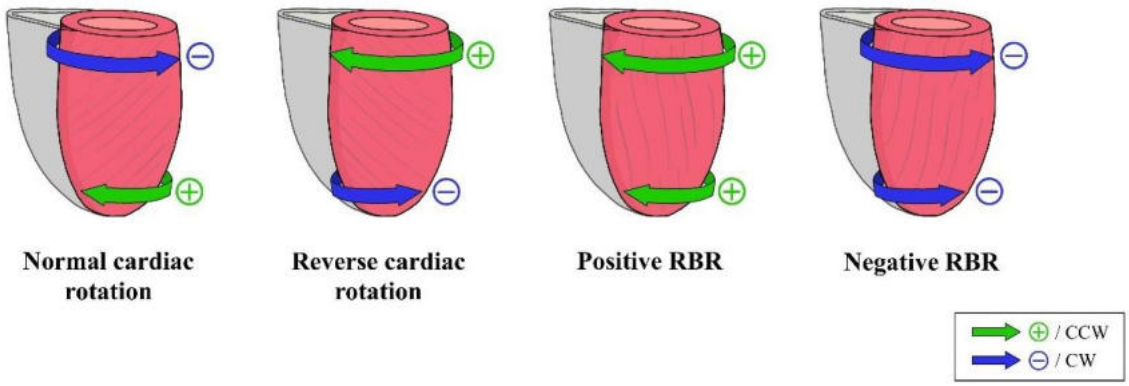

Figure 7: The four types of cardiac rotation *(71). Normal rotation with positive apical and negative basal rotation; reverse rotation with negative basal and positive apical rotation; positive RBR with positive apical and basal rotation and negative RBR with negative apical and basal rotation, respectively. CCW = counterclockwise, CW = clockwise, RBR = rigid body rotation.*

Although these abnormal rotational patterns may be a marker of cardiac maturation impairment (72), positive RBR was also described in healthy individuals (70, 73). Negative RBR has been identified as an indicator of subclinical mechanical impairment in several cardiovascular diseases; however, it was most strongly associated with LVNC, particularly in cases with HF (73-80).

1.2.4 Genetic analysis

Considering the new guidelines that emphasize the role of the etiological aspects rather than the morphological ones, genetic testing has become an important part of LVNC diagnosis (10, 16, 81).

The analysis of previously CMP-related mutations is recommended in symptomatic LVNC in order to confirm the diagnosis, to provide information about the prognosis and

reproductive management, and to affect the treatment of the patient eventually (10). According to Petersen et al., genetic testing should not be performed in asymptomatic hypertrabeculated phenotype individuals with otherwise normal cardiac findings (10).

After the identification of a causative mutation, the genetic analysis of the first-degree relatives is also recommended (10).

1.3 Problem statement – left ventricular hypertrabeculation: what is the myth behind the phenotype?

Although several research has been conducted in recent years to address the questions of left ventricular hypertrabeculation and noncompaction, the recent changes in the international guidelines have again highlighted the uncertainties surrounding this issue (10, 16).

Numerous data are available in the literature regarding LVNC with decreased LVEF and severe cardiovascular complications, which the ESC and Petersen statements refer to as LVNC with CMP and provide information about its diagnosis and clinical management (10, 16). Similarly, the novel recommendations distinguish the asymptomatic excessive trabeculated phenotype with otherwise normal cardiac findings and preserved LVEF and entitle it as a normal morphological variant (without further need for clinical follow-up) (10, 16).

However, we should highlight the lack of evidence about symptomatic LVNC with preserved LVEF. Regarding this grey zone excessive trabeculated phenotype, less research was conducted, and also mainly questions and no indications are stated in the abovementioned recommendations (10, 16). No precise information is available about the genetic background, clinical characteristics and outcome, follow-up, and prognostic factors in symptomatic LVNC with preserved LVEF. Meanwhile, the risk stratification of LVNC individuals may be useful. In addition, there are few recommendations available as current studies were mainly conducted on LVNC patients with HF (10, 43, 44).

2. Objectives

The present work aimed to investigate the different forms of hypertrabeculation by using the TB post-processing CMR method and to evaluate the functional, rotational, genetic, and clinical characteristics of symptomatic excessive trabeculation phenotype with preserved LVEF.

2.1 Different methods, different results? Threshold-based versus conventional contouring techniques in clinical practice

Although both the CC and TB techniques are accepted by the Society for Cardiovascular Magnetic Resonance post-processing guidelines, the differing TPMi evaluation — which leads to variations in clinical diagnosis, risk stratification, and therapeutic decisions — has not been previously studied (55). Moreover, despite the validation at a 70% threshold, the optimal adjustment of the TB method is not well-defined (56, 57, 59). Thus, we aimed to evaluate the differences in LV and RV volumetric, functional, and muscle mass parameters measured with CC and TB post-processing methods at 70% and 50% thresholds in different hypertrabeculated conditions. Our further purpose was to assess this clinical impact of these differences.

2.2 Genetic, clinical and imaging implications of a noncompaction phenotype population with preserved ejection fraction

Although the genetic determination and clinical characteristics of LVNC with decreased LVEF and cardiovascular complications are well described in the literature, the genetic background of symptomatic excessive trabeculation with preserved LVEF was not studied before (10, 16, 35-38, 82). Thus, we aimed to characterize the genetic background and clinical manifestation of symptomatic LVNC with preserved LVEF, to analyze the connection between genotype, clinical presentation, and phenotype by using CMR modality, and to compare the CMR values with a healthy control (C) group.

2.3 The effect of excessive trabeculation on cardiac rotation - a multimodal imaging study

Abnormal cardiac rotational patterns, especially negative RBR, were associated with LVNC with HF and cardiovascular complications (10, 16). However, cardiac rotational impairment has not previously been studied in relation to genetic heterogeneity. Thus, we

aimed to investigate cardiac rotation in a symptomatic LVNC phenotype population with preserved LVEF and control individuals and aspire to analyze the relation of cardiac rotation to LVNC genotype and functional values. Additionally, we aimed to describe the intermodality agreement of cardiac rotational parameters between CMR-ST and Echo-ST methods.

3. Methods

3.1 Study populations and study design

All procedures performed in these three studies were in accordance with the 1964 Helsinki Declaration and its later amendments or comparable ethical standards. Ethical approval was obtained from the Central Ethics Committee of Hungary, and all participants provided informed consent.

3.1.1 Study populations and study design when comparing the threshold-based and conventional contouring methods

This retrospective study included 30 DCM and 30 ACM patients, 30 LVNC phenotype individuals, 30 healthy athletes, and 30 healthy C persons from a Caucasian population. The baseline characteristics are reported in **Table 1**.

Patients with dilated LV, increased LV volume, decreased LV function (LVEF<50%) and without a known cause of LV dysfunction were included in the DCM group (83). The ACM group enrolled patients with a definite diagnosis of ACM, which was established if two major or one major and two minor or four minor Task-Force criteria were present (29). The revised Task-Force criteria evaluate the imaging, pathological, genetic and clinical aspects, ECG recordings and family history of ACM patients (29). Hypertrabeculated phenotype individuals, who fulfilled the Petersen criteria (TL/CL ratio > 2.3) and had at least one clinical manifestation e.g. HF, arrhythmia, positive family history, were enrolled in the LVNC group (84). Healthy athletes with more than 10 hours per week of mixed training activity (mean ± SD: 20.0 ± 4.2 hours/week), with no symptoms, normal sports cardiology assessment, and normal ECG were enrolled in the athletes group (20). The control group enrolled healthy volunteers without relevant cardiovascular or extracardiac diseases.

We excluded patients with ischemic, valvular, and congenital heart diseases, other or overlapping CMP, relevant comorbidities such as hypertension or diabetes mellitus, and individuals with a sports activity more than 6 hours per week (except in athletes). Additionally, technical reasons e.g. implanted devices, artifacts, and contrast agent administration before segmentation, were the other exclusion criteria (85).

Table 1: Baseline characteristics of the study populations when analyzing the CC and TB methods with 70% and 50% thresholds (63). *ACM = arrhythmogenic cardiomyopathy, BMI = body mass index, BSA = body surface area, DCM = dilated cardiomyopathy, LVNC = left ventricular noncompaction, p = significance level of the ANOVA test, * =p<0.05. Values represent mean ± standard deviation.*

	Total population	**LVNC**	**ACM**	**DCM**	**Athletes**	**Healthy volunteers**	**p**
Population (n)	150	30	30	30	30	30	0.523
Men (n)	80	15	18	17	15	15	0.889
Age (years)	39.8±15.8	43.4±13.5	44.0±17.1	50.7±14.7	23.0±3.7	37.6±11.0	<0.001*
BSA (m^2)	1.9±0.2	1.9±0.3	1.9±0.2	2.0±0.2	1.9±0.2	1.9±0.2	0.141
BMI (kg/m^2)	25.3±4.5	26.2±5.2	25.0±4.2	28.2±5.0	23.7±2.3	23.3±3.8	<0.001*

3.1.2 Study populations and study design when analyzing the genetic, clinical and imaging background of a noncompaction phenotype population with preserved ejection fraction

This cross-sectional study included 54 symptomatic LVNC phenotype individuals with preserved LVEF and 54 sex-and age-matched control subjects from a Caucasian population. Baseline characteristics are listed in **Table 2**.

The LVNC group enrolled symptomatic persistent isolated hypertrabeculated phenotype subjects who fulfilled the Petersen (TL/CL>2.3) and Jacquier (LVTPMi >20% of the LVTMi) LVNC criteria on CMR images and have preserved LVEF (>50%) (52, 84). Healthy individuals without known cardiac or extracardiac diseases and an exercise activity <6 hours per week were enrolled in the control group (20).

Our exclusion criteria included patients with reduced LVEF (<50%), congenital, ischemic, or valvular diseases, other or overlapping CMP, hypertension, relevant cardiac and extracardiac comorbidities, exercise activity >6 hours per week or other known cause

of transient hypertrabeculation and technical reasons, e.g. implanted cardiac devices, artifacts or contrast agent administration before segmentation (20, 85).

Table 2: Baseline characteristics of the study populations when evaluating the genetic and clinical background of LVNC (45). *BMI = body mass index, BSA = body surface area, LVEF = left ventricular ejection fraction, LVNC = left ventricular noncompaction, VUS = variant of uncertain significance, p = significance level of the student t-test and ANOVA test, * =p<0.05 significance between the LVNC and control groups. Values represent mean ± standard deviation.*

	Control group	**Total LVNC population**	**p**	**Genetic subgroups**			
				Benign	**VUS**	**Pathogenic**	**p**
Population (n)	54	54	1.000	11	30	13	0.488
Men (n)	33	33	1.000	7	20	6	0.391
Age (years)	38±14	39±14	0.743	42±15	39±13	36±16	0.592
BMI (kg/m^2)	24.3±3.0	25.2±4.2	0.148	25.3±4.3	26.1±4.4	23.4±3.1	0.157
BSA (m^2)	1.9±0.2	2.0±0.2	0.183	2.0±0.2	2.0±0.2	1.8±0.2	0.158
LVEF (%)	69±5	65±5	<0.01*	66±3	64±6	65±5	0.758

3.1.3 Study populations and study design when examining the cardiac rotation in excessive trabeculation with preserved cardiac function

This retrospective study included 54 symptomatic LVNC phenotype subjects with preserved LVEF and 54 sex-and age-matched healthy volunteers from a Caucasian population. CMR examination was performed in all participants and echocardiography examination was conducted in 39 LVNC and 40 control subjects. The baseline characteristics are presented in **Table 3.**

The LVNC group included symptomatic persistent, isolated excessive trabeculated phenotype subjects, who fulfilled the Petersen and Jacquier criteria, have preserved LVEF on CMR images (LVEF>50%), and a cardiogenetic examination was performed before (10, 52). Patients with reduced LVEF (<50%) on CMR images, congenital, ischemic, or

valvular diseases, transient or secondary hypertrabeculation, other or overlapping CMP, relevant cardiac or extracardiac comorbidities e.g. hypertension, diabetes mellitus or chronic renal disease were excluded from the LVNC group. The control group enrolled healthy individuals without known cardiovascular or extracardiac diseases. Another exclusion criteria in the LVNC and control groups were the >6 hours per week of physical activity and technical reasons, e.g., artifacts or contrast agent administration before segmentation on CMR images (20, 85).

Table 3: Baseline characteristics of the study populations when investigating the cardiac rotation of LVNC and control populations (71). *BMI = body mass index, BSA = body surface area, CMR = cardiac magnetic resonance imaging, Echo = echocardiography, LVNC = left ventricular noncompaction, VUS = variant of uncertain significance, p = significance level of the student t-test and ANOVA test, * =p<0.05. Values represent mean ± standard deviation.*

	Control	**LVNC**	**p**	**Pathogenic**	**VUS**	**Benign**	**p**
CMR study population (n)	54	54	1.000	15	27/	12	0.402
Men (n)	33	33	1.000	7	18	8	0.400
Available Echo data (n)	40	39	1.000	9	21	9	0.523
Age (years)	38.7±15.1	40.0±13.9	0.834	38.5±17.0	40.0±12.4	42.0±14.1	0.813
BSA (m^2)	1.9±0.2	2.0±0.2	0.062	1.8±0.2	2.0±0.2	2.0±0.2	0.093
BMI (kg/m^2)	23.9±3.4	25.3±4.2	0.072	23.4±3.3	26.3±4.5	25.4±4.2	0.096

3.2 Cardiac magnetic resonance imaging - image acquisition and analysis

CMR examinations were conducted in a similar manner across all three studies, as presented in this chapter.

Image acquisition

The 1.5 T MRI scanners were used to perform the CMR examinations: Magnetom Aera, Siemens Healthineers, Erlangen, Germany, and Achieva, Philips Medical System, Eindhoven, the Netherlands. Retrospectively gated, balanced steady-state free precession (bSSFP) cine sequences were performed with short-axis (SA) and two-, three-, and four-chamber long-axis (LA) views from base to apex, covering the whole LV and RV. The slice thickness was 8 mm with no interslice gap, and the field of view was 350 mm on average, adapted to body size.

In the abovementioned studies, healthy volunteers and athletes do not receive contrast agent. A contrast agent (gadobutrol 0.1 mL/kg, gadobenate 0.2 mL/kg or gadoterate 0.2 mL/kg) was administered to 76 patients in the first study (24 LVNC, 27 DCM, 25 ACM patients) and 50 LVNC individuals in the second and third studies (13 P, 27 variant of unknown significance - VUS and 10 B genotype subjects). In order to provide the best image quality for post-processing analysis, the administration of the contrast agent was performed after the acquisition of the SA cine images (85). The contrast-enhanced images were acquired approximately 10 minutes after the administration of the contrast agent.

Image analysis

The Medis Suite software (Medis Medical Imaging Systems, Leiden, the Netherlands) was used for CMR post-processing analysis. In the first study, the volumetric and functional parameters were analyzed by using both the CC and TB post-processing methods, while the second and third studies included only the TB values.

Firstly, the manual correction of the semiautomatic endo- and epicardial borders was performed on end-diastolic and end-systolic SA images from base to apex in both the LV and RV. Using the CC technique, the area within the endocardial contour was assessed as blood volume, and between the epi-and endocardial borders was counted as myocardial mass. The TPMi can not be evaluated separately with the CC method, and it is counted as part of the blood volume. Values calculated with the CC technique were interpreted only in the first study.

Thereafter, the TB algorithm (Massk module of Medis Suite software) was applied. Whereas the TB method is based on the different signal intensities of the myocardium

and blood, it can identify each voxel within the epicardial border as part of the myocardial mass or blood volume. Using the TB method, the voxels identified as myocardium between the epi- and endocardial borders were classified as TMi and within the endocardial border as TPMi. The first study analyzed values with both 70% and 50% thresholds, and the second and third studies reported only 50% threshold parameters.

In the third study, we also assessed manually the thickness of the CL (CLT) in end-diastolic CMR images of the LV in two-, three- and four-chamber LA views, following the AHA-17 segment model (excluding the segment 17 – apex) and recommendations from prior studies (84, 86).

In addition, the commercially available FT method of Medis Suite software (QStrain, version 4.1) was used for deformation analysis in the second and third studies. The previously described SA (for rotational parameters) and manually traced two-, three- and four-chamber LA endocardial contours (for strain measurements) were tracked by the CMR-FT algorithm and followed throughout the cardiac cycle (64, 87). Following the standard recommendations, the basal slice was selected at the level of the mitral valve, and the apical slice was detected well beyond the papillary muscles on SA images (65). In the third study, the available echocardiographic images were also considered when selecting the basal and apical slices in order to enhance the standardization of CMR-FT and Echo-ST rotation measurements.

3.3 Echocardiography – image acquisition and analysis

Echocardiography was performed only in the third study, as described in this chapter.

Valuable echocardiography images performed at the same medical check-up as the CMR examinations were available at 39 LVNC (9 P, 21 VUS, and 9 B) and 40 control subjects. 2D transthoracic echocardiography was conducted by using a GE Vivid E95 instrument with a 4Vc-D phased-array transducer (GE Vingmed Ultrasound, Horten, Norway). ECG-gated apical two-, three- and four-chamber LA images and LV-focused parasternal SA images were acquired at the mitral valve and apical levels with a target frame rate of more than 50 frames per second. For post-processing analyses, we used the 2D Tomtec Cardiac Performance Analysis software (Philips Ultrasound Workspace, TOMTEC Imaging

Systems GmbH, Unterschleissheim, Germany). After selecting the optimal heart cycle, the automatically generated end-diastolic and end-systolic LV endocardial contours were manually corrected. The LV functional parameters were calculated from the LA images. The speckle-tracking algorithm (Echo-ST), which tracks each intramyocardial speckle between the endo- and epicardial contours from frame to frame through the cardiac cycle, was applied to SA images for the determination of cardiac rotational data (65, 69).

3.4 Studied parameters

3.4.1 Studied parameters when comparing the threshold-based and conventional contouring methods

The following LV and RV parameters were determined with the CC technique and TB method using 70% and 50% thresholds: end-diastolic, end-systolic, and stroke volume (EDV, ESV, SV), EF, end-diastolic TM and TPM. All parameters were indexed (i) to body surface area (BSA). The Alfakih normal values were considered as a reference in the CMP and C populations, and the 95th percentile ranges in the athletes (88, 89).

3.4.2 Studied parameters when analyzing the genetic, clinical and imaging background of a noncompaction phenotype population with preserved ejection fraction

In this study the following LV and RV parameters were calculated and indexed to BSA (i) using the TB method: EDVi, ESVi, SVi, EF, TMi, TPMi. By using the CMR-FT method, we also measured the LV GLS and GCS values and interpreted them as absolute values: when a parameter is closer to zero, it represents a poorer LV function, and when farther from zero, it represents a better LV function. The Alfakih normal values for adults and the percentiles by Kawel-Boehm for children were used as a reference for the functional and the normal values described by Peng et al. for the strains (13, 88). The clinical manifestation of LVNC was evaluated through parameters described as the „red flag” system (subheading 3.6.2).

3.4.3 Studied parameters when examining the cardiac rotation in excessive trabeculation with preserved cardiac function

The following LV functional parameters were calculated both with the CMR TB method and echocardiography: EDV, ESV, SV, and, EF. Additionally, the LVTM and LVTPM muscle mass values were determined by CMR. All parameters were indexed to BSA (i) and the Alfakih and Kawel-Boehm normal values were used as a reference (13, 88). The CLT was measured in all AHA-17 segments (except segment 17), and the mean CLT values were determined at the apical, mid-ventricular, and, basal levels.

Cardiac rotation was assessed both with CMR-FT and Echo-ST quantitatively by measuring the endocardial end-systolic peak rotation at basal and apical levels and qualitatively by the positive (CCW) or negative (CW) direction of rotation (69). For the quantitative evaluation of overall cardiac rotation, the net cardiac twist parameter was calculated as the absolute difference between the apical and basal rotation (65, 69, 90, 91). The following cardiac rotational patterns (described in subsection 1.2.3) were also differentiated: normal rotation, reverse rotation, and positive and negative RBR (**Figure 7**).

3.5 Genetic testing

After genetic counseling, peripheral venous blood samples were collected from LVNC subjects for genetic testing by using next-generation sequencing (NGS) with a 174-gene panel (TruSight Cardio Sequencing Kit, Illumina, USA). This method detects single-nucleotide variations and small insertions/deletions in genes previously associated with cardiac diseases without identifying large mutations. Sequencing produced paired-end reads (150 nucleotides in length), and data were analyzed by using FastQC (v0.11.9), MultiQC (v1.9), BWA (v0.7.12), and GATK (v4.1.7.0) software and with manual variant screening. The hg19 (GRCh37.p13) genome was used as a reference.

The detected variants were classified, and the clinical relevance was evaluated as per American College of Medical Genetics and Genomics (ACMG) guidelines by using the Franklin, VarSome, ClinVar, ClinGen, and OMIM genetic databases (81). Based on this information, pathogenic (P), likely pathogenic (LP), VUS, likely benign, and benign mutations were distinguished.

In the second study, we divided LVNC subjects based on the detected CMP-related mutations into three subgroups: the P subgroup with P or LP mutations, the VUS subgroup with VUS mutations, and the benign (B) subgroup without relevant genetic mutations (on 01.12.2022). CMP-related mutations were further grouped into two subtypes: directly LVNC-related when associated with "excessive trabeculation" and other CMP-related mutations, which may have a pathogenic role due to genetic overlap with other CMP (28).

Considering the dynamic aspect of genetic information, mainly due to the reclassification of VUS mutations, in the third study, we redistributed the LVNC subgroups based on the refreshed genetic data in databases (on 01.11.2023.).

3.6 Clinical evaluation

3.6.1 Clinical evaluation when comparing the threshold-based and conventional contouring methods

When evaluating the clinical decisions using the different post-processing methods, the currently available guidelines and recommendations were applied in each patient population and athletes (22, 25, 29, 43, 52, 92-95). The changes in clinical diagnosis, risk stratification, and therapy, derived from the measured differences in LV and RV parameters with CC and TB techniques, were noted.

3.6.2 Clinical evaluation when analyzing the genetic, clinical and imaging background of a noncompaction phenotype population with preserved ejection fraction

Clinical data were collected through questionnaires during cardiogenetic counseling for LVNC subjects and during CMR examinations for the control group. Family history focused on hereditary cardiac diseases, arrhythmias, SCD, recurrent loss of consciousness and implanted cardiac devices. The personal medical history covered symptoms (syncope, dizziness, atypical chest pain, palpitations); ischemic or structural heart diseases; arrhythmias; SCD; thromboembolic events; implanted cardiac devices; other metabolic, gastrointestinal, hepatic, nephrology, endocrine, autoimmune, neurologic, oncologic and psychiatric comorbidities and sports activity. Additionally, clinical

information was supplemented by personal clinical genetic counseling and data from the electronic medical records.

Risk factors and adverse clinical endpoints were identified as “red flags” based on the available literature data to enhance the clinical assessment. These included a family history of CMP or SCD in first-degree relatives (referred to as positive family history); increased LVEDVi on CMR; ventricular tachycardia or fibrillation; ECG abnormalities (left bundle branch block – LBBB or inverted T waves); unexplained syncope, thromboembolism, SCD in the personal history and nonischemic mid-myocardial or subepicardial LGE (13, 37, 43, 44, 60, 61, 88, 96). Additionally, an episode of minor reduction in LVEF (up to 45%) that normalized quickly with treatment was also considered a red flag (60).

3.6.3 Clinical evaluation when examining the cardiac rotation in excessive trabeculation with preserved ejection fraction

The study population of the second and third studies is identic, therefore, the clinical data was listed and presented under subheadings 4.2 and 5.2.

3.7 Statistical analysis

Continuous variables are presented as mean ± standard deviation (SD) or as median with interquartile range, while categorical variables are expressed as frequencies and percentages. The homogeneity of variances was evaluated using Levene’s test, and distribution normality was assessed using the Shapiro–Wilk test. Quantitative differences between the two populations were assessed by using independent t-tests for normally distributed data and Mann–Whitney U tests for non-normal distributions. For comparisons within the same group, paired Student’s t-tests or Wilcoxon tests were applied. For analyses involving three or more groups, ANOVA with Tukey’s post hoc test was used for normally distributed variables with equal variances, the Welch test with the Games-Howell *post hoc* test for unequal variances, and the Kruskal–Wallis test for non-normally distributed data. Bonferroni correction was applied for multiple comparisons. Qualitative data were compared by using the chi-square test or Fisher’s exact test. Correlations were evaluated by using the Pearson correlation coefficient. In the third study, intermodality agreement between CMR and echocardiography was evaluated

using the Bland-Altman analysis. Cohen's kappa, with the chi-square test, was used to assess the strength of association regarding the direction of rotation. Interobserver agreement was assessed by using the intraclass correlation coefficient (ICC). Statistical significance was defined as a p-value <0.05. Data analysis was performed by using IBM SPSS Statistics (version 28.0, Armonk, NY).

4. Results

4.1 Results of comparing the threshold-based and conventional contouring methods

Interobserver agreement

The interobserver agreement between the three observers was described as excellent with a global ICC of 0.988 (0.958-0.997) for CC, 0.991 (0.973-0.997) for TB 70% and 0.992 (0.974-0.998) for TB 50% measurements.

Analyzing the trabeculation of study populations

In hypertrabeculated conditions, LVTPMi was significantly higher with both the 70% and 50% TB setups in all the cardiomyopathy groups and athletes compared to the control group (**Figure 8**).

Comparing LV and RV parameters measured with CC and TB methods

The comparison of the CC and TB techniques revealed that the TB method (at both 70% and 50% thresholds) resulted in lower LV and RV EDVi and ESVi but higher TMi across all groups. While LV and RV SVi were generally lower with the TB technique, significant differences were mainly observed in LVSVi for LVNC subjects, athletes, and control group and in RVSVi for DCM, LVNC, and control groups. The LV and RV EF were significantly higher with the TB method, except for RVEF in the DCM group, where no significant difference was found. Details are presented in **Table 4**.

Table 4: Comparing the LV and RV parameters measured with conventional contouring and threshold-based methods with 70% and 50% thresholds (63). *ACM = arrhythmogenic cardiomyopathy, DCM = dilated cardiomyopathy, LV = left ventricular, RV = right ventricular, EDVi = left ventricular end-diastolic volume index, EF = left ventricular ejection fraction, ESVi = left ventricular end-systolic volume index, LVNC = left ventricular noncompaction, SVi = left ventricular stroke volume index, TMi = left ventricular total mass index. Values represent mean ± standard deviation. Bold values of p indicate statistical significance of ANOVA test, p<0.05; ¶ = p<0.05 TB method at 70%*

versus conventional contouring; # = p<0.05 TB 50% method versus conventional contouring.

LVNC										
	LV					RV				
	EDVi (ml/m^2)	**ESVi** (ml/m2)	**SVi** (ml/m2)	**EF** (%)	**TMi** (g/m2)	**EDVi** (ml/m2)	**ESVi** (ml/m2)	**SVi** (ml/m2)	**EF** (%)	**TMi** (g/m2)
CC	120.57 ± 32.23¶#	71.74 ± 32.99¶#	48.83 ± 8.28¶#	43.33 ± 12.94¶#	53.97 ± 15.77¶#	82.54 ± 13.86¶#	36.65 ± 9.13¶#	45.89 ± 6.52¶#	56.09 ± 5.46¶#	13.07 ± 2.15¶#
TB 70%	86.29 ± 21.32¶	43.07 ± 21.81¶	43.23 ± 7.73¶	52.90 ± 14.88¶	89.96 ± 28.45¶	62.41 ± 10.66¶	23.47 ± 6.46¶	38.94 ± 5.56¶	62.94 ± 5.74¶	34.20 ± 6.59¶
TB 50%	86.75 ± 21.31#	43.17 ± 21.82#	43.58 ± 7.72#	53.02 ± 14.84#	89.48 ± 28.50#	62.77 ± 10.69#	23.53 ± 6.46#	39.24 ± 5.55#	63.06 ± 5.62#	33.82 ± 6.53#
p	**<0.001**	**<0.001**	**0.011**	**0.011**	**<0.001**	**<0.001**	**<0.001**	**<0.001**	**<0.001**	**<0.001**
ACM										
CC	106.32 ± 15.54¶#	53.24 ± 12.90¶#	53.07 ± 10.01	50.15 ± 8.14¶#	42.92 ± 6.70¶#	121.70 ± 20.77¶#	75.75 ± 24.49¶#	47.02 ± 10.48¶#	38.82 ± 10.47¶#	19.32 ± 3.24¶#
TB 70%	79.92 ± 12.93¶	32.26 ± 10.53¶	47.65 ± 9.49	59.92 ± 9.74¶	70.60 ± 10.58¶	101.15 ± 15.78¶	56.69 ± 22.25¶	45.49 ± 11.07¶	45.50 ± 13.49¶	40.61 ± 8.36¶
TB 50%	80.80 ± 13.04#	32.26 ± 10.53#	48.53 ± 9.57	60.36 ± 9.62#	69.68± 10.60#	102.02 ± 15.92#	56.69 ± 22.25#	46.40 ± 11.10#	45.96 ± 13.41#	39.69 ± 8.18 #
p	**<0.001**	**<0.001**	0.73	**<0.001**	**<0.001**	**<0.001**	**<0.001**	0.86	**0.01**	**<0.001**
DCM										
CC	153.57 ± 40.92¶#	111.99 ± 37.89¶#	41.58 ± 8.98	28.27 ± 7.29¶#	71.09 ± 21.32¶#	82.85 ± 24.12¶#	39.38 ± 17.15¶#	41.25 ± 8.95¶#	52.30 ± 12.59	14.18 ± 4.08¶#

TB 70%	111.82 ± 33.36¶	75.14 ± 28.97¶	36.68 ± 8.56	34.24 ± 7.94¶	114.92 ± 29.64¶	60.34 ± 17.24¶	25.69 ± 11.59¶	32.94 ± 8.86¶	56.79 ± 14.15	36.95 ± 9.75¶
TB 50%	112.45 ± 33.47#	75.32 ± 29.12#	37.13 ± 8.64	34.47 ± 7.93#	114.27 ± 29.51#	60.76 ± 17.40#	25.75 ± 11.56#	33.25 ± 9.01#	56.92 ± 14.09	36.51 ± 9.65#
p	**<0.001**	**<0.001**	0.61	**0.003**	**<0.001**	**<0.001**	**<0.001**	**<0.001**	0.332	**<0.001**
Athletes										
CC	117.55 ± 11.06¶#	53.92 ± 7.67¶#	63.63 ± 9.75¶#	54.03 ± 5.57¶#	56.31 ± 8.97¶#	108.54 ± 12.00¶#	53.61 ± 7.34¶#	54.94 ± 8.42	50.54 ± 4.81¶#	22.46 ± 2.22¶#
TB 70%	87.58 ± 9.55¶	31.70 ± 6.15¶	55.88 ± 8.99¶	63.70 ± 6.27¶	87.80 ± 10.75¶	88.20 ± 11.46¶	33.95 ± 5.04¶	54.25 ± 9.23	61.31 ± 4.82¶	43.60 ± 4.51¶
TB 50%	87.82 ± 9.44#	31.80 ± 6.19#	56.02 ± 8.80#	63.70 ± 6.22#	87.17 ± 10.64#	88.74 ± 11.64#	34.27 ± 5.22#	54.47 ± 9.06#	61.21 ± 4.70#	42.74 ± 3.88#
p	**<0.001**	**<0.001**	**0.002**	**<0.001**	**<0.001**	**<0.001**	**<0.001**	0.955	**<0.001**	**<0.001**
Healthy volunteers										
CC	84.80 ± 12.23¶#	33.67 ± 6.73¶#	51.13 ± 8.51¶#	60.34 ± 4.86¶#	45.64 ± 7.76¶#	84.09 ± 12.26¶#	36.05 ± 8.22¶#	48.67 ± 8.94¶#	57.58 ± 6.10¶#	15.27 ± 3.46¶#
TB 70%	65.77 ± 9.58¶	20.59 ± 4.74¶	45.18 ± 6.79¶	68.81 ± 4.71¶	65.62 ± 11.11¶	66.21 ± 10.70¶	24.93 ± 6.41¶	41.98 ± 8.73¶	62.77 ± 6.47¶	33.97 ± 5.78¶
TB 50%	65.88 ± 9.54#	20.72 ± 4.75#	45.17 ± 6.73#	68.67 ± 4.69#	65.50 ± 11.12#	66.31 ± 10.69#	25.01 ± 6.40#	42.00 ± 8.75#	62.70 ± 6.50#	33.86 ± 5.80#
p	**<0.001**	**<0.001**	**0.005**	**<0.001**	**<0.001**	**<0.001**	**<0.001**	**0.005**	**0.002**	**<0.001**

Comparing the 70% and 50% TB thresholds

No significant differences were observed in LV and RV volumetric, functional, or TMi parameters between the 70% and 50% thresholds of the TB method across all groups (**Table 4**). However, TPMi values were significantly higher in all groups when using the 70% threshold compared to the 50% threshold (**Figure 8**).

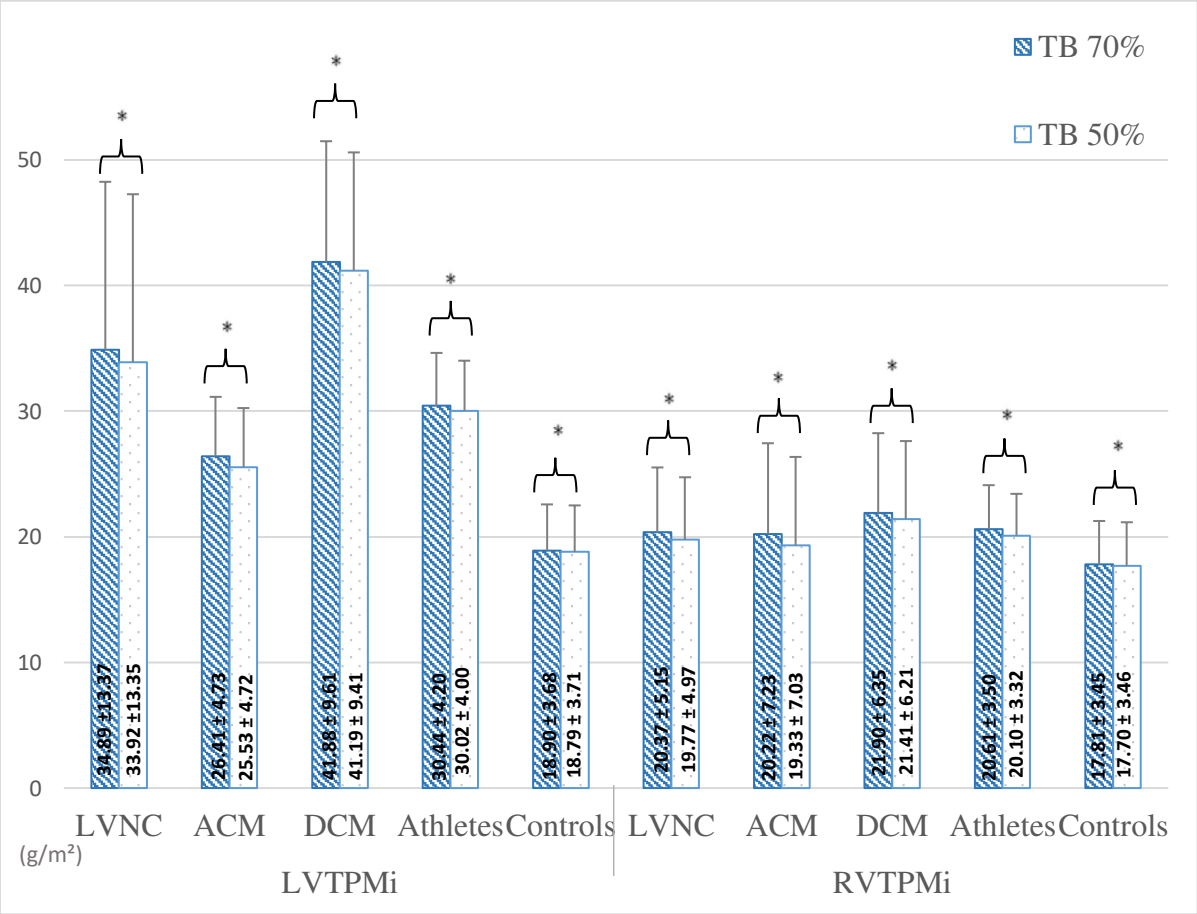

Figure 8: The LV and RV trabeculated and papillary muscle mass values measured with threshold-based method at 70% and 50% thresholds in all study populations (63). *LVNC = left ventricular noncompaction, ACM = arrhythmogenic cardiomyopathy, DCM = dilated cardiomyopathy, LV = left ventricle, RV = right ventricle, TPMi = trabeculated and papillary mass index, TB = threshold based, * =p<0.05, statistical significance of the student t-test, values represent mean ± standard deviation.*

Analyzing the clinical impact of the CC or TB methods

Regarding the clinical impact of using different post-processing methods, we evaluated how the differences in functional and muscle mass parameters influence the diagnosis, risk stratification, and therapeutic decisions in the studied hypertrabeculated populations. In the LVNC group, the TB technique impacted all these aspects: TPMi was required for the diagnosis in all cases, and other factors were affected in about 30% of the cases. In the ACM group, the TB method could alter diagnostic Task-Force criteria in 67% of patients, could deny diagnosis in 17%, reduce the need for pharmaceutical therapy in 33% and eliminate the need for an ICD in one case. Among DCM patients, therapy indications were modified in 34%, and the estimated risk for mortality or transplantation decreased in two cases. For three asymptomatic athletes meeting Petersen and Jacquier LVNC criteria, the TB method normalized LVEF above 50%. Detailed findings are provided in **Table 5**.

Table 5: Modification effect of the threshold-based method with both 70% and 50% threshold setups in clinical decision making – detailed data (a) and summary (b) (63). *ACM = arrhythmogenic cardiomyopathy, CRT-D = cardiac resynchronization therapy with defibrillator, DCM = dilated cardiomyopathy, HFmrEF = heart failure with mid-range ejection fraction, HFrEF = heart failure with reduced ejection fraction, LVEDVi = left ventricular end-diastolic volume index, LVEF = left ventricular ejection fraction, LVNC = left ventricular noncompaction, LVTPMi = left ventricular trabeculated and papillary muscle mass index, RVEDVi = right ventricular end-diastolic volume index, RVEF = right ventricular ejection fraction, TB = threshold-based.*

a)	**What does the TB method modify?**	**Clinical impact**	**n / %**
LVNC (n= 30)	quantification of LVTPMi	verify Jacquier diagnostic criteria	30 / 100
	reduction in LVEDVi	reduction in the risk of complications	10 / 33
	improvement in LVEF	reclassification from HFrEF to HFmrEF-pharmacotherapeutic changes	8 / 27

		reduction in the primary prophylactic criteria for anticoagulation	8 / 27
		reduction of CRT-D implantation indication	9 / 30
ACM (n= 30)	reduction in RVEDVi or/and improvement in RVEF	loss of ACM diagnosis	8 / 27
		loss of major Task-Force criteria	6 / 20
		reduction of major to minor Task-Force criteria	6 / 20
		loss of minor Task-Force criteria	5 / 17
	improvement in LVEF	reclassification from HFmrEF to preserved EF-pharmacotherapeutic changes	7 / 23
		reclassification from HFrEF to HFmrEF-pharmacotherapeutic changes	3 / 10
		reduction of CRT-D implantation indication	1 / 3
DCM (n= 30)	improvement in RVEF	reduction in the risk of mortality and cardiac transplantation	2 / 7
	improvement in LVEF	reclassification from HFrEF to HFmrEF-pharmacotherapeutic changes	5 / 17
		rejection of CRT-D implantation indication	5 / 17
Athletes (n= 30)	improved LVEF	falls out from partial sport restriction	3 / 10

b)	**Diagnostic criteria evaluation**	**Risk stratification**	**Pharmacotherapy**	**Device therapy**
LVNC (n/%)	30 / 100	10 / 33	8 / 27	9 / 30
ACM (n/%)	17 / 56	0	10 / 33	1 / 3
DCM (n/%)	0	2 / 7	5 / 17	5 / 17
Athletes (n/%)	3 / 10	0	0	0
Healthy volunteers (n/%)	0	0	0	0

4.2 Results of analyzing the genetic, clinical and imaging background of a noncompaction phenotype population with preserved ejection fraction

Interobserver agreement

The interobserver agreement between the two observers was excellent with a global ICC of 0.958 (0.830-0.990) for LV, 0.976 (0.905-0.994) for RV parameters and 0.955 (0.888-0.983) for LV strains.

Genetic classification of the LVNC group

Thirteen (24%) LVNC subjects were categorized in the pathogenic subgroup, carrying likely pathogenic or pathogenic CMP-associated mutations. Among these, 46% had heterozygous mutations in TTN, 15% in MYH7, and 8% each in TNNT2, MYBPC3, MIB1, RYR2, SCN5A, and KCNQ1. In one person two pathogenic mutations were present in different genes (TTN and RYR2). The VUS subgroup included 56% (30 subjects) with VUS in CMP-associated genes, TTN mutations being the most frequent (29%). The remaining 20% (11 subjects) without relevant CMP-associated mutations were classified in the B subgroup. Detailed genetic data are listed in the supplementary material of the published manuscript (45).

Subjects with pathogenic and VUS mutations were further divided into two genetic subtypes: those who have at least one mutation previously directly linked to LVNC and those who only have mutations in CMP-related genes. Ninety-two percent of the pathogenic and 77% of the VUS subgroup had directly LVNC-related mutations (**Figure 10**).

Comparing the CMR parameters between the LVNC and control groups

The LVNC group showed significantly increased LVEDVi, LVESVi, LVTMi, and LVTPMi, and significantly decreased LVEF, GLS, and GCS compared to the C population; however, all functional parameters remained in the normal range. No significant differences were observed in LVSVi and RV parameters between the two groups. Results are presented in **Figure 9**.

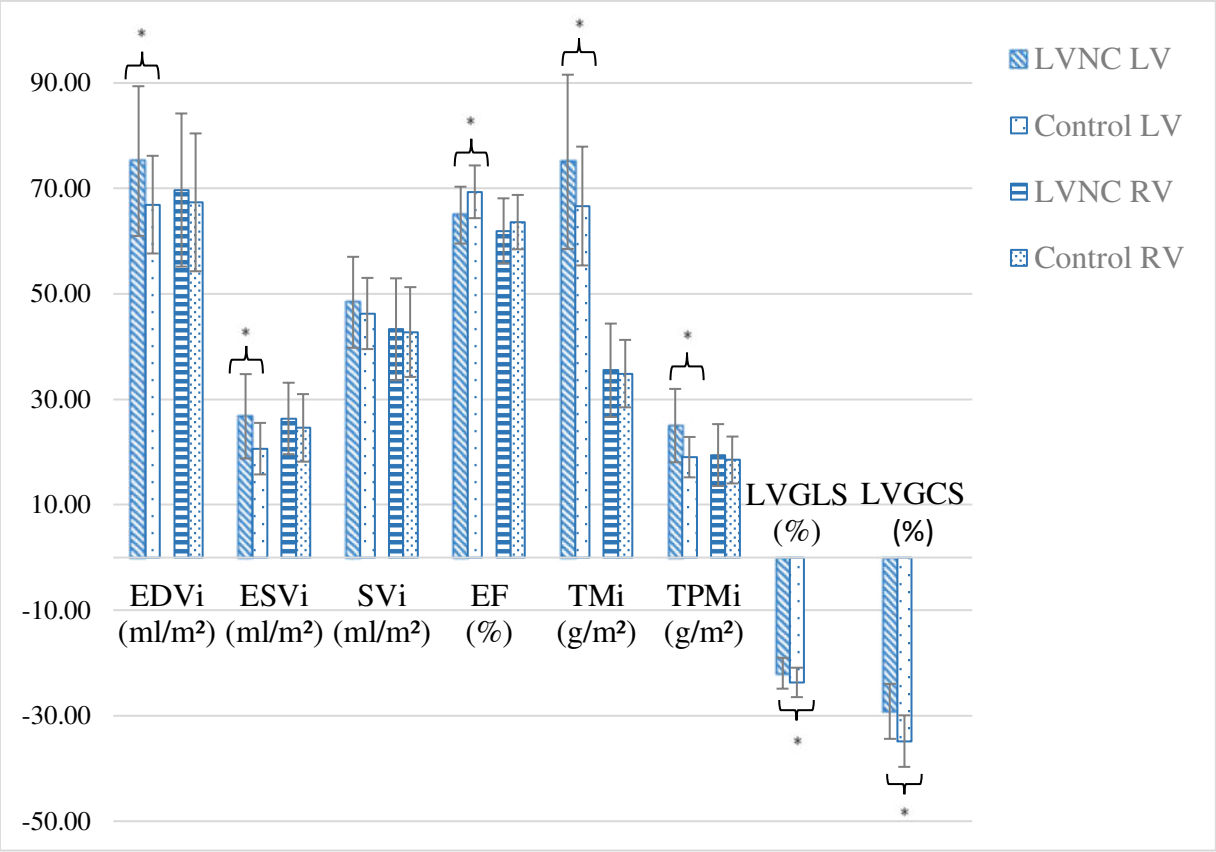

Figure 9: Comparing the LV and RV functional and strain parameters in the LVNC and control populations (45). *LVNC = left ventricular noncompaction, LV = left ventricle, RV = right ventricle, EDVi = end-diastolic volume index, ESVi = end-systolic volume index, SVi = stroke volume index, EF = ejection fraction, TMi = total mass index, TPMi = trabeculated and papillary mass index, GLS = global longitudinal strain, GCS = global circumferential strain, * =p<0.05 statistical significance of student t-test.*

Comparing the CMR parameters among the LVNC genetic subgroups

The LV and RV functional and LV strain parameters were comparable among the genetic LVNC subgroups (**Table 6**).

Table 6: Comparing the LV and RV functional and strain parameters among the three LVNC genetic subgroup (45). *LVNC = left ventricular noncompaction, LV = left ventricle, RV = right ventricle, EDVi = end-diastolic volume index, ESVi = end-systolic volume index, SVi = stroke volume index, EF = ejection fraction, TMi = total mass index, TPMi = trabeculated and papillary mass index, GLS = global longitudinal strain, GCS = global circumferential strain, VUS = variant of unknown significance, p=ns*

	Pathogenic (n=13)	VUS (n=30)	Benign (n=11)	p
LVEDVi	77.0 ± 15.9	75.4 ± 14.0	72.5 ± 13.5	0.748
LVESVi	26.8 ± 8.1	27.1 ± 8.4	25.9 ± 7.4	0.911
LVSVi	50.1 ± 9.8	48.3 ± 8.5	46.7 ± 7.9	0.622
LVEF	65.4 ± 5.2	64.5 ± 6.2	65.8 ± 2.6	0.758
LVTMi	75.0 ± 16.1	76.9 ± 18.0	70.0 ± 12.4	0.498
LVTPMi	26.1 ± 6.6	25.4 ± 7.9	22.7 ± 4.1	0.442
LVCMi	48.9 ± 10.7	51.5 ± 12.2	47.3 ± 10.4	0.545
RVEDVi	70.2 ± 15.9	68.9 ± 14.5	71.3 ± 14.2	0.889
RVESVi	26.3 ± 6.1	26.1 ± 7.1	27.0 ± 7.3	0.935
RVSVi	43.9 ± 11.7	42.7 ± 9.0	44.2 ± 9.7	0.874
RVEF	62.1 ± 5.9	61.9 ± 6.2	62.1 ± 7.0	0.989
RVTMi	34.8 ± 7.9	36.4 ± 10.0	34.1 ± 6.6	0.726
RVTPMi	19.4 ± 5.8	20.2 ± 6.4	17.4 ± 4.0	0.418
GLS	-21.4 ± 3.4	-22.0 ± 2.8	-22.3 ± 2.9	0.759
GCS	-29.2 ± 4.2	-28.6 ± 5.4	-30.8 ± 5.9	0.487

Analyzing the clinical characteristics of LVNC subgroups

When comparing the clinical manifestation of LVNC among the genetic subgroups, the positive family history of CMP or SCD and the personal medical history of thromboembolism were significantly higher in the pathogenic and VUS subgroups. SCD and elevated LVEDVi were observed only in the pathogenic subgroup, while temporary LVEF reduction, inverted T waves on ECG, and LGE on CMR were present in the pathogenic and VUS subgroups. Arrhythmias occurred at similar rates across all subgroups except ventricular tachycardia, which was slightly more prevalent in subjects with genetic involvement. Atrioventricular nodal reentry tachycardia (AVNRT) was noted in two subjects from the VUS subgroup. Despite these observations, most parameters were statistically comparable across the groups. Interestingly, atypical chest pain was significantly more frequent in the B subgroup. Childhood LVNC diagnosis occurred in 13% of the cohort: 4 P, 2 VUS and 1 B subjects. Results are provided in **Table 7**.

Table 7: Clinical characteristics of the pathogenic, VUS and benign LVNC genetic subgroups (45). *AVNRT = atrioventricular nodal reentry tachycardia, CMR = cardiac magnetic resonance imaging, ECG = electrocardiogram, LBBB = left bundle branch block, LGE = late gadolinium enhancement, LVEDVi = left ventricular end-diastolic volume indexed to body surface area, LVEF = left ventricular ejection fraction, LVNC = left ventricular noncompaction, VES = ventricular extrasystole, VUS = variant of uncertain significance, = part of the red flag risk stratification model, * =p<0.05 statistical significance of Chi-square test.*

		Genotypes of LVNC population			
		Pathogenic (n=13)	**VUS (n=30)**	**Benign (n=11)**	**p**
	Diagnosed in childhood	4	2	1	0.094
	Positive family history	8	15	1	0.024*
Subjects' symptoms	Unexplained syncope	2	2	1	0.816
	Dizziness	6	15	8	0.355
	Atypical chest pain	5	7	8	0.014*
	Palpitations	7	15	6	0.954
Arrhythmia	Nondocumented arrhythmia	3	5	2	0.894
	Documented arrhythmia	5	13	5	0.935
	Supraventricular arrhythmia	3	7	1	0.661
	Atrial fibrillation	0	3	1	0.638
	Ventricular arrhythmia	5	10	5	0.77
	VES	4	9	4	0.925
	Ventricular tachycardia	2	2	1	0.816
	Bradycardia	1	1	1	0.579
	AVNRT	0	2	0	0.497
Negative endpoints	Thromboembolic event	2	0	0	0.038*
	Sudden cardiac death	1	0	0	0.201
ECG signs	T wave inversion	3	5	0	0.235
	LBBB	1	0	1	0.231

CMR parameters	↑ LVEDVi	2	0	0	0.093
	Temporary LVEF ↓	1	4	0	0.698
	LGE	2	2	0	0.671

Describing the „red flag" system

The three genetic subgroups differed significantly regarding the presence and number of red flags per individual (**Figure 10**). A moderate positive correlation between the number of red flags per individual and genotype was described (r=0.457, p=0.01).

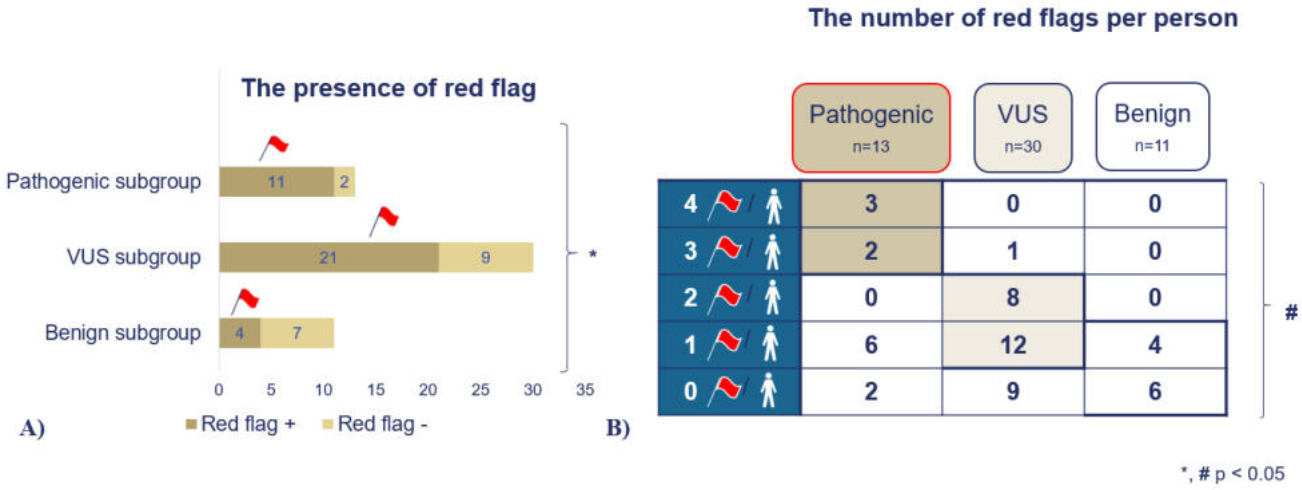

Figure 10: Analyzing the presence (A) and number (B) of red flags in the three LVNC genetic subgroups (45). *CMP = cardiomyopathy, LVNC = left ventricular noncompaction, n = number of subjects, VUS = variant of uncertain significance, * = p < 0.05, the significance level of the chi-square test on the presence of red flags among the three genetic subgroups, # = p < 0.05, the significance level of the ANOVA test on the number of red flags among the three genetic subgroups.*

Interestingly, the number of red flags was significantly higher in individuals with directly LVNC-related mutations compared to those with other CMP-related mutations (p<0.001); and a moderate positive correlation was observed between the number of red flags and the presence of LVNC-related mutations (r=0.407, p=0.01).

Individuals with LVNC-associated pathogenic mutations exhibited the highest number of red flags per person; typically, 1–2 red flags were present in the VUS subgroup, while those in the B subgroup had none or only a single red flag. Details are presented in **Figure 11**.

4.3 Results of examining the cardiac rotation in excessive trabeculation with preserved cardiac function

Interobserver agreement

The interobserver agreement between the two observers was moderate to excellent with a global ICC of 0.977 (0.932-0.992) for CMR functional, 0.830 (0.513-0.942) for CMR rotational, 0.910 (0.724-0.969) for Echo functional and 0.755 (0.412-0.918) for Echo rotational parameters.

Comparing the functional and rotational values between the LVNC and control groups

In the LVNC population, significantly higher LVEDVi, LVESVi, LVTMi and LVTPMi were described, along with lower LVEF and apical CLT, compared to the C group. CMR-FT analysis revealed significantly reduced apical rotational degree and net cardiac twist in the LVNC group, with no difference in basal rotation. Echo-ST results showed no significant differences in rotational values between the groups. Results are presented in **Table 8**. The direction of rotation was similar at the basal level, whereas a negative (CW) rotation at the apical level was only observed in the LVNC group (**Table 9**).

Comparing the functional and rotational values among the LVNC genetic subgroups

The functional parameters and quantitative rotational values measured both with CMR and echocardiography were comparable among the P, VUS and B genetic subgroups, whereas mid and apical CLT differed significantly (**Table 8**).

However, the presence of negative (CW) apical rotation was higher in subjects with genetic involvement, no significant differences were noted in the direction of basal rotation across the LVNC subgroups (**Table 9**).

Table 8: Comparing the CMR and echocardiography functional and rotational parameters among the study populations (71). *CLT = compact layer thickness, CMR =*

cardiac magnetic resonance imaging, Echo = echocardiography, LV = left ventricle, EDVi = end-diastolic volume index, EF = ejection fraction, ESVi = end-systolic volume index, LVNC = left ventricular noncompaction, SVi = stroke volume index, TMi = total myocardial mass index, TPMi = trabeculated and papillary mass index, n = number of the study group, NA = not applicable, VUS = variant of uncertain significance, Values represent mean ± standard deviation, bold p values indicate statistical significance of student t-test and ANOVA test, p<0.05.

CMR							
	Control	**LVNC**	**p**	**Pathogenic**	**VUS**	**Benign**	**p**
LVEDVi (ml/m^2)	67.7±10.7	74.4±14.6	**0.007**	75.5±18.5	74.9±13.3	72.0±13.0	0.807
LVESVi (ml/m^2)	20.8± 4.9	26.6± 8.3	**<0.001**	27.2±10.6	26.8±7.4	25.2±7.4	0.81
LVSVi (ml/m^2)	46.8±7.7	47.9±8.9	0.508	48.2±10.3	48.1±8.9	46.8±7.5	0.893
LVEF (%)	69.3±4.8	64.7±6.0	**<0.001**	64.6±6.8	64.4±6.1	65.4±5.4	0.902
LVTMi (g/m^2)	65.9±10.6	74.4±16.2	**0.004**	73.6±18.4	77.0±16.6	69.7±11.9	0.417
LVTPMi (g/m^2)	19.8±4.7	25.1±7.1	**<0.001**	26.4±8.4	25.4±7.3	22.6±3.9	0.369
Basal CLT (mm)	6.5±0.6	6.4±0.7	0.515	6.1±0.7	6.6±0.7	6.5±0.8	0.081
Mid CLT (mm)	5.9±0.4	5.7±0.7	0.070	5.3±0.9	5.9±0.5	5.9±0.5	**0.009**
Apical CLT (mm)	5.4±0.2	4.8±0.8	**<0.001**	3.9±0.7	5,0±0.5	5.3±0.3	**<0.001**
Basal rotation (°)	-5.1±6.5	-3.5±7.1	0.209	-1.0±5.8	-5.0±6.7	-3.1±8.8	0.207

Apical rotation (°)	12.3±9.3	6.7±11.0	**0.005**	8.1±10.8	3.4±10.1	12.2±11.6	0.058
Net cardiac twist (°)	17.9±10.9	12.4±9.7	**0.006**	10.3±9.8	11.8±8.0	16.3±12.3	0.262
ECHO							
LVEDVi (ml/m^2)	66.4±13.6	73.0±15.1	**0.047**	67.5±19.3	75.0±15.0	73.5±11.0	0.509
LVESVi (ml/m^2)	29.0±7.6	34.6±7.7	**<0.001**	31.2±9.0	35.6±8.1	35.4±5.4	0.389
LVSVi (ml/m^2)	38.3±7.3	38.4±7.9	0.950	36.3±10.8	39.4±7.4	38.1±6.1	0.653
LVEF (%)	57.9±5.0	52.7±2.7	**<0.001**	53.6±3.4	52.7±2.6	51.8±2.2	0.385
Basal rotation (°)	-5.4±4.2	-5.0±6.6	0.740	-4.6±6.0	-5.8±6.4	-3.5±7.9	0.662
Apical rotation (°)	5.7±5.0	3.8±5.5	0.106	4.9±5.3	3.6±6.5	3.0±3.0	0.769
Net cardiac twist (°)	11.0±6.2	10.0±7.7	0.508	9.9±7.3	10.3±8.9	9.1±5.3	0.922

Table 9: Comparing the direction of basal and apical rotation in the control group and LVNC genetic subgroups. *CW = clockwise, CCW = counterclockwise, LVNC = left ventricular noncompaction, CMR = cardiac magnetic resonance imaging, echo = echocardiography, VUS = variant of unkown significance. * = p < 0.05 significance level between the LVNC and control group or among the three genetic subgroups.*

CMR							
	Control	**LVNC**	**p**	**Pathogenic**	**VUS**	**Benign**	**p**
Basal	CW:45, CCW:9	CW:40, CCW:14	0.240	CW:9, CCW:6	CW:23, CCW:4	CW:8, CCW:4	0.164
Apical	CW:0, CCW:54	CW:15, CCW:39	0.001*	CW:5, CCW:10	CW:10, CCW:17	CW:0, CCW:12	<0.05*
ECHO							
Basal	CW:38, CCW:2	CW:33, CCW:6	0.126	CW:7, CCW:2	CW:20, CCW:1	CW:6, CCW:3	0.094
Apical	CW:0, CCW:40	CW:10, CCW:29	0.001*	CW:1, CCW:8	CW:8, CCW:13	CW:1, CCW:8	0.224

Analyzing the correlations of cardiac rotation

In the LVNC group, apical rotation and net cardiac twist (measured by both CMR-FT and Echo-ST) showed a moderate positive correlation with age and a moderate negative correlation with LVEDVi, LVESVi and LVSVi when assessed by CMR-FT. Additionally, CMR-FT net cardiac twist had a moderate negative correlation with LVTPMi. Basal rotational degrees measured by either method did not show significant correlations. Interestingly, none of the measured rotational degrees showed a significant correlation with genotype.

In the control group, the only significant association was a positive correlation between Echo-ST apical rotation and age. Detailed data are presented in **Table 10.**

Table 10: Correlating the rotational data with age, functional parameters and genotype in the LVNC and C populations using CMR-FT (a) and Echo-ST (b) (71). *C = control group, CLT = compact layer thickness, CMR-FT = cardiac magnetic resonance feature-tracking method, Echo-ST = speckle-tracking echocardiography, LV = left ventricle, EDVi = end-diastolic volume index, EF = ejection fraction, ESVi = end-systolic volume index, LVNC = left ventricular noncompaction, SVi = stroke volume index, TMi = total myocardial mass index, TPMi = trabeculated and papillary mass index, NA = not applicable, r = Pearson correlation coefficient, * = p<0.05.*

a)	**CMR-FT basal rotation** (°)		**CMR-FT apical rotation** (°)		**CMR-FT net cardiac twist** (°)	
	LVNC	**C**	**LVNC**	**C**	**LVNC**	**C**
Age (years)	-0.09	0.29*	0.35*	0.14	0.36*	-0.05
LVEDVi (ml/m^2)	0.10	-0.29*	-0.37*	-0.09	-0.42*	0.05
LVESVi (ml/m^2)	0.10	-0.35*	-0.32*	-0.14	-0.30*	0.01
LVSVi (ml/m^2)	0.06	-0.19	-0.30*	-0.02	-0.41*	0.07
LVEF (%)	-0.07	0.24	0.13	0.13	0.04	0.01
LVTMi (g/m^2)	0.04	-0.21	-0.18	-0.06	-0.19	0.03
LVTPMi (g/m^2)	0.09	-0.20	-0.26	-0.18	-0.35*	-0.05
Basal CLT (mm)	-0.02	0.04	0.11	-0.04	0.05	-0.07
Mid CLT (mm)	0.02	-0.06	0.20	0.04	0.16	0.06
Apical CLT (mm)	-0.15	-0.07	0.07	0.01	0.19	0.02

b)	**Echo-ST basal rotation** (°)		**Echo-ST apical rotation** (°)		**Echo-ST net cardiac twist** (°)	
	LVNC	**C**	**LVNC**	**C**	**LVNC**	**C**
Age (years)	-0.11	-0.37*	0.38*	0.16	0.35*	0.35*
LVEDVi (ml/m^2)	0.02	-0.03	-0.22	-0.03	-0.13	0.02
LVESVi (ml/m^2)	0.04	-0.06	-0.25	-0.15	-0.15	-0.05
LVSVi (ml/m^2)	-0.01	0.01	-0.19	0.09	-0.11	0.08
LVEF (%)	-0.17	0.07	0.09	0.31	0.14	0.17

Analyzing the cardiac rotational patterns

The control group presented a normal rotational pattern and positive RBR across both modalities. In the total LVNC population, rotational patterns included normal (52%), positive RBR (20%), negative RBR (22%), and reverse rotation (6%).

LVNC subjects in the B subgroup displayed predominantly normal patterns and positive RBR, except for one case with negative RBR on Echo-ST analysis. In contrast, the VUS and pathogenic subgroups showed all four rotational patterns with negative RBR at approximately one-third to one-fourth of the population. Additionally, a reverse rotational pattern was identified in three subjects (two pathogenic and one VUS) by using CMR-FT. In these cases, Echo-ST data was not available. Detailed data on cardiac rotational patterns is presented in **Figure 11**.

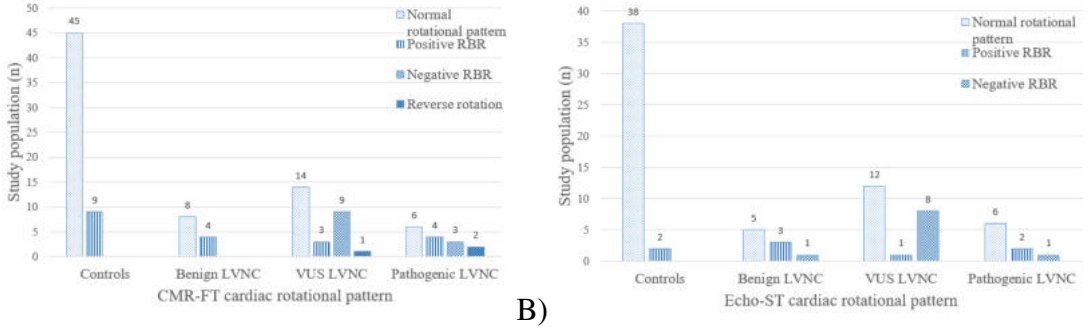

A) B)

Figure 11: The distribution of cardiac rotational patterns across the control group and the three LVNC genetic subgroup with CMR-FT method (image A) and Echo-ST technique (image B) (71). *CMR-FT = cardiac magnetic resonance imaging feature-tracking method, Echo-ST = speckle-tracking echocardiography, LVNC = left ventricular noncompaction, VUS = variant of unkown significance, RBR = rigid body rotation.*

Intermodality comparison of CMR-FT and Echo-ST methods

The intermodality comparison of CMR-FT and Echo-ST rotational values revealed no significant correlation or agreement for apical, basal, and net quantitative values in either the LVNC or control groups (**Table 11**).

Table 11: Comparing the CMR-FT and Echo-ST rotational degrees – correlations and Bland-Altman analysis (71). *C = control group, CMR-FT = cardiac magnetic resonance imaging feature-tracking method, Echo-ST = speckle-tracking echocardiography, LVNC = left ventricular noncompaction, Bias = the mean value of the difference between the CMR-FT and Echo-ST methods, LOA = limit of agreement, the mean value of the difference between the two methods ± 2SD, bold p values indicate statistical significance = p<0.05.*

CMR-FT versus Echo-ST	Correlation r (p)		Bland-Altman analysis					
			Bias		p		95% LOA	
	LVNC	C	LVNC	C	LVNC	C	LVNC	C
Basal rotation (°)	0.33 (0.039)	-0.08 (0.626)	1.46	0.19	0.243	0.884	-13.90; 16.82	-15.91; 16.28
Apical rotation (°)	0.11 (0.496)	0.34 (0.031)	2.75	5.91	0.179	**<0.001**	-22.37; 27.88	-10.88; 22.70
Net cardiac twist (°)	0.15 (0.366)	0.36 (0.022)	2.19	6.53	0.239	**<0.001**	-19.99; 24.23	-13.92; 26.97

However, the qualitative values as basal and apical direction and cardiac rotational pattern demonstrated moderate to good association between the two methods: Cohen's kappa in the LVNC group: basal 0.65, apical 0.60 and net cardiac twist 0.65, $p<0.05$ and Cohen's kappa in the control group: basal 0.40, apical 1.0, net cardiac twist 0.40, $p<0.05$.

5. Discussion

5.1 Discussions of comparing the threshold-based and conventional contouring methods

In this study, we analyzed the differences and their clinical implications in LV and RV functional and muscle mass parameters between the CC technique and TB method in different hypertrabeculated and control populations.

Despite the differences between the TB and CC techniques, both methods were validated before and could be used in clinical practice according to the Society for Cardiovascular Magnetic Resonance post-processing guideline (55). Namely, Jasper et al. demonstrated good correlations of the TB method with a dynamic heart phantom model, and the TB technique correlated well with histological findings regarding the muscle mass measurements (56, 97). Additionally, validation of SVi with aortic flow measurements indicated that the TB method aligned closely with aortic flow, both showing significant deviations from the CC method (59).

Comparative studies on healthy populations have shown similar results to ours for LV and RV parameters between the CC and TB methods namely the TB method calculated lower volumetric parameters and higher EF and TMi values (57, 58). Similar observations were also reported in various cardiovascular conditions and healthy individuals when several manual contouring techniques were compared, differing in calculating TPMi to the blood volume or to the myocardial muscle mass (51, 98, 99).

In our investigation, all the measured parameters were comparable between the 70% and 50% setup of theTB method, except TPMi being significantly higher at 70%, although this difference did not result in any clinical impact in this study population. To the best of our knowledge, no specific recommendation determines the optimal threshold configuration of the TB method, and limited research has focused on comparing different thresholds. Jaspers et al. applied a 70% threshold when validating the TB method against the heart phantom model. However, they noted this setup might be high, as the phantom model cannot totally mimic the normal physiology (56). The validation by Varga-Szemes

et al. was at the 50% threshold, and this setup is the most common in everyday clinical practice (59).

In the literature, a few studies highlighted the potential relevance of using the TB method in various pathologies, as significant changes could occur when measuring parameters with the TB method and establishing diagnosis, risk stratification, and therapeutic decisions based on conventional guidelines (56, 57, 100). Despite the retrospective nature of our study, we also intended to analyze how the TB method can influence the clinical assessment of our patients.

Regarding the diagnostic implications, the TB method provided an effective approach to evaluate the Jacquier criteria by quantifying TPMi in the LVNC group. Thus, alongside the previously established Petersen criteria, a more precise differential diagnosis of LVNC can be established by differentiating it from physiological hypertrabeculation (43, 52, 84). Similarly, applying the TB method in the ACM group resulted in decreased RVEDVi and higher RVEF, impacting the major and minor CMR criteria of the revised Task-Force guidelines (29). In some cases, these adjustments prompted a reevaluation of the diagnosis, particularly in ACM with mild clinical manifestation, which suggests that the TB method may assist in diagnosing borderline ACM cases, though no supporting literature exists. Similarly, adjustments to LVEDVi and LVEF might potentially influence DCM diagnoses; however, we reported no changes in our study (83). Regarding diagnosing hypertrabeculation in athletes, the guideline by Pelliccia et al. recommends restricting athletes with LVNC and near-normal LVEF from high-intensity sports, while hypertrabeculated phenotype with normal LVEF and without symptoms should not be classified as LVNC (22, 25). Four athletes from our study population fell into the restricted category; however, the TB method normalized LVEF in three of them, removing the restrictions. Thus, bringing volumetric and functional values of athletes closer to the normal population with the TB method, the TB technique could aid in differentiating physiological hypertrabeculation from the pathological forms.

The impact of the TB method on the prognostic assessment of LVNC individuals may include lowering the estimated risk of adverse cardiovascular events and reducing the need for further investigation or genetic testing by measuring increased LVEF and decreased LVEDVi (43, 60). In addition, the estimated risk of mortality or cardiac

transplantation was influenced in the DCM group by calculating higher RVEF with the TB method, which is an important part of risk stratification (95).

Considering the therapeutic aspects, the pharmaceutical and device therapy were both affected by reclassifying HF severity after TB measurements: from HFmrEF to preserved EF and from HFrEF to HFmrEF in all three patient groups (LVNC, ACM, DCM). Reclassification from HFmrEF to preserved EF might delay treatment initiation, while the indication of several new drugs is dedicated to the HFrEF patient population (93). Furthermore, anticoagulation therapy is recommended for LVNC patients with LVEF below 40% in order to address blood stasis in intertrabecular recesses; thus, the LVEF improvement via the TB method could postpone therapy initialization (6, 41, 101). Although several aspects influence the indication of ICD or cardiac resynchronization therapy, LVEF below 35% is a main criterion, and in our study, the improved LVEF with TB method altered this decision in 15 CMP patients (93). The described clinical aspects align with prior studies by using manual contouring methods (51, 98).

To summarize, the examples above emphasize the importance of careful evaluation of the hypertrabeculated phenotype and highlight the need for updated diagnostic criteria in these cases.

5.2 Discussions of analyzing the genetic, clinical and imaging background of a noncompaction phenotype population with preserved ejection fraction

In this study, we compared the LVNC population to healthy volunteers, analyzed the genetic background of LVNC with preserved LVEF, and evaluated the genotype-phenotype associations throughout the presentation of the red flag system.

Comparing the LVNC and control groups, our results aligned with the literature as LV volumetric and muscle mass parameters were significantly higher and the LVEF and strain values were lower in the LVNC group. However, all the studied CMR parameters remained within the normal range (17, 67, 102). Regarding RV metrics, we did not observe significant differences between the two groups, in contrast to Kiss et al. describing higher RV volumes and RVTMi in LVNC patients (102).

Our results showed comparable CMR parameters across the three LVNC genetic subgroups, unlike previous studies that linked pathogenic genotype to LV systolic dysfunction and some studies also to the extent of trabeculation (17, 37, 60, 62, 82, 103, 104). This discrepancy may derive from differences in study populations, as previous research included LVNC with both preserved and reduced LVEF, focusing on LVNC patients with HF. Notably, no prior data specifically focused on LVNC with preserved LVEF, making our findings a novel contribution to this area.

Regarding the genetic background of LVNC, previous studies reported the same mutations with similar or slightly higher rates of genetic involvement, as observed in our findings (10, 37, 38, 105). The slightly higher rate of pathogenic mutations in these studies could be attributed to the heterogenous LVNC study populations. Furthermore, the occurrence of pathogenic genotype was even higher (87.5%) in LVNC patients needing heart transplantation and children with LVNC (35-37, 106, 107). This is in line with our results, as genetic involvement was more common in those diagnosed in childhood.

Previous studies in the literature identified certain clinical characteristics as prognostic factors in LVNC, although these elements were not analyzed together before (13, 37, 60, 61, 88, 96). However, literature reviews by Vergani et al. and Negri et al. propose the need for a complex risk stratification system in LVNC (43, 44). The novelty of our study is the creation of the "red flag" system, which combines imaging and clinical factors and demonstrates a statistical association between red flags and genotype. Furthermore, no previous studies examined the genotype-phenotype relationship in LVNC with preserved LVEF.

Major cardiovascular complications, namely thromboembolic events, ventricular arrhythmias, and HF symptoms, are often linked to systolic dysfunction and pathogenic genotype in the literature (35, 38, 43, 44, 60, 82). Although, as our results demonstrate, complications could occur even with preserved LVEF. Our findings revealed a significantly higher prevalence of thromboembolic events and a positive family history of CMP or SCD in the pathogenic and VUS LVNC subgroups, whereas SCD occurred in one case with pathogenic mutations. Although additional clinical characteristics, such as

unexplained syncope, ventricular tachycardia or fibrillation, inverted T waves on the ECG, LBBB, LGE, elevated LVEDVi, and a transient reduction in LVEF showed no significant associations with the presence of genetic mutations, we incorporated them into our risk stratification model, as the prognostic role of these factors has been demonstrated by previous studies (13, 37, 43, 44, 60, 61, 88, 96). For example, repolarisation abnormalities such as inverted T waves and LBBB were associated with cardiovascular events, and syncope has been highlighted as an early indicator of ventricular arrythmia (34, 35, 38, 42-44, 96, 108-110). Interestingly, the importance of the pathogenic mutations in the development of various types of ventricular and supraventricular arrhythmias has been shown in some studies, whereas others report higher occurrence of LBBB in sporadic LVNC cases than in genetically determined ones (34, 35, 37, 38, 44, 96, 110). Elevated LVEDVi, transient LVEF reductions, and LGE were recognized as predictors of poor outcome and LVNC-specific complications (60). Consistent with our findings, where we detected LGE only in subjects with CMP-related mutations, LGE has often been associated with pathogenic mutations in the literature (61, 62, 103). It is worth mentioning that symptoms such as dizziness and palpitations were similarly distributed across LVNC genetic subgroups, and atypical chest pain had a higher prevalence in the B subgroup. This underlines the subjective nature of these symptoms and reduces their role in risk stratification.

As mentioned before, the existence of a comprehensive risk stratification approach, like our red flag model, is preferred over the individual evaluation of each clinical parameter. Although this idea was mentioned in the literature theoretically, its clinical application and relationship with genetic background were not quantified yet before (43, 44). As a novel perspective in the literature, we reported not only a higher prevalence but also a higher number of red flags per individual in subjects with pathogenic genotype. Individuals with multiple red flags had a higher probability of carrying genetic mutations, whereas LVNC subjects without CMP-related mutations had no or only one red flag. Thus, red flags might facilitate clinical patient management, the indication of genetic testing and allowing a more flexible follow-up strategy for individuals without red flags (10). Our results align with the “Expert Consensus Statement on the state of genetic testing for cardiac diseases” by describing similar clinical elements as indicators of genetic testing (111). Further notable results emphasize the specific aspects of excessive

trabeculated phenotype as we identified significantly more red flags per individual in carriers of LVNC-specific mutations than in those with other CMP-related mutations.

Additionally, it is worth mentioning that the clinical and imaging characteristics of the VUS subgroup were between the B and P subgroups, typically exhibiting one or two red flags per person. The interpretation of VUS mutations is challenging in routine practice, whereas the ACMG guideline recommends against considering VUS as a clinical-decision-making mutation (16, 81). Our results suggest that additional monitoring during follow-up may be necessary for these cases as with new data, reclassification of VUS mutations could occure in ACMG databases.

5.3 Discussions of examining the cardiac rotation in excessive trabeculation with preserved cardiac function

In this study, we investigated the cardiac rotation measured with CMR-FT and Echo-ST methods in LVNC subjects with preserved LVEF and in controls.

Comparing the LVNC and control groups, the significantly higher volumetric and muscle mass values and lower LVEF and apical CLT in the LVNC population align with existing literature (17, 67). The basal rotation was comparable between the two groups, which is consistent with the literature, although a reduction in basal rotation was described in LVNC with HF (73, 76, 77, 91, 112, 113). In contrast, we identified reduced apical rotational degree and net cardiac twist in our LVNC study population compared to controls, and negative (CW) apical rotation was present only in this group. Similar results have been reported in relatives of LVNC patients, mildly hypertrabeculated individuals, healthy athletes and HF patients (74-77, 91, 113-116). However, literature presenting no differences in net cardiac twist between hypertrabeculated and control subjects is also available (79). This phenomenon could be explained by the fact that apical rotation and cardiac twist increased in a dose-dependent manner following dobutamine infusion and decreased after esmolol infusion, whereas basal rotation remained unchanged in studies on animal models (117). Furthermore, apical rotation was found to be more closely related to contractility (dP/dt) than LVEF, and twist has an important effect on cardiac function in HF patients (74, 114, 115, 117). These data suggest that abnormal apical rotation may serve as a subclinical indicator of contractility impairment, as the rotation

of subendocardial fibers plays a critical role in maintaining EF, especially in the apical segment. The negative correlations between rotational parameters and LVTPMi and volumetric parameters in our study demonstrate the connection between hypertrabeculation and rotational changes. Moreover, the importance of analyzing apical movement in clinical practice is emphasized by literature data as abnormal apical rotation was described as an independent predictor of cardiovascular complications, and hypertrabeculated HF patients are also characterised by deteriorated apical strain values (66, 68, 73).

When analyzing the LVNC genetic subgroups, the functional parameters were comparable among the three subgroups measured both with CMR and echocardiography. Although previous studies have highlighted a connection between impaired LVEF and genotype (36, 37), such associations have not been explored before in LVNC subjects with preserved LVEF. A reduced CLT at mid and apical segments was observed in genetically determined LVNC, aligning with recent findings linking CLT <5 mm in these segments to LVNC with reduced LVEF (86). In terms of cardiac rotation, no differences were reported in rotational degrees among the genetic subgroups; however, a notable difference was identified in the direction of apical rotation, namely, negative CW apical rotation occurred only in LVNC individuals with pathogenic or VUS genotype. According to the available scientific literature, this is the first study to compare cardiac rotation in LVNC morphology subjects across different genotypes.

Regarding cardiac rotational patterns, the normal variant predominated in the control group, with a small proportion exhibiting positive RBR, a variant previously reported in healthy individuals without a clear understanding of its significance (73, 79, 118). Our findings align with literature data in terms of the total LVNC population, namely approximately half of them displayed a normal rotational pattern, whereas one-fifth had positive RBR; and 30% showed negative RBR or reverse rotation (73, 76, 79, 91, 113, 114). Furthermore, negative RBR was previously linked to impaired LV function and is considered a hallmark of hypertrabeculation, and associated with cardiovascular complications, advanced heart failure, and myocardial fibrosis (76, 77, 80, 119). Additionally, LVNC patients with negative RBR had longer QRS intervals, higher rates of LBBB, and lower LVEF than those with positive RBR (77, 78). Considering LVNC

genetic subgroups, our study is the first to examine cardiac rotational patterns across genotypes. Normal rotation was found in two-thirds of B genotype individuals, whereas one-third exhibited positive RBR. Analyzing the VUS and pathogenic subgroups, RBR was observed in almost half of the population, primarily as a negative pattern, with almost 10% showing reverse rotation. In the literature, abnormal cardiac rotation was identified in LVNC patients with a positive family history, and RBR was reported in about one-third of first-degree relatives and hypertrabeculated individuals with a positive family history (78, 113, 114).

Finally, we performed the intermodality comparison of CMR-FT and Echo-ST methods and reported no strong correlation or reasonable agreement regarding rotational degrees, with CMR-FT calculating higher values. These findings are in line with previous studies highlighting CMR-FT's tendency to overestimate and Echo-ST's tendency to underestimate parameters compared to tagging imaging (90, 120). Similarly, quantitative strain analysis has also shown poor agreement between CMR-FT and Echo-ST, though they correlated well for volume measurements (121-123). Notably, no prior research specifically compared these methods for cardiac rotation measurements in excessive trabeculated populations. The differences in rotational values between the two methods can be attributed to different technical approaches: CMR-FT tracks the endocardial border in three dimensions, while Echo-ST follows intramyocardial features in two dimensions (64). Despite this, moderate to good agreement was observed in evaluating the direction and pattern of rotation, suggesting that these parameters may have broader applicability across modalities. Although cardiac rotation can be assessed by using either technique in clinical practice, our results suggest that these modalities are not interchangeable. Thus, follow-up and serial measurements should be performed consistently using the same method to ensure comparability.

5.4 Limitations

We need to mention the limitations of our studies. The TB method, used in all three studies, has its own limitations as it quantifies from short-axis slices with an 8 mm spatial resolution in the Z-direction. This can result in partial volume effects due to the non-perpendicular alignment of trabeculae and papillary muscles, potentially affecting the

measurements. The first study was cardiac imaging-focused, thus the clinical data of the studied patients was limited. Regarding the second and third studies, their cross-sectional and retrospective nature limited the longitudinal insights, and the smaller sample size of genetic sub-groups may have affected the statistical findings. Additionally, the 174-gene panel used in these studies, though extensive, may not cover all variants, and novel updates to the ACMG databases could reclassify VUS findings over time. Finally, although CMR-FT and Echo-ST are validated for clinical research, their accuracy depends on protocol adherence and should be used by experienced observers.

6. Conclusions

Although excessive trabeculation has been the focus of recent studies and recommendations, there are still many questions surrounding this issue, especially in the case of hypertrabeculation with preserved LVEF. This dissertation aimed to answer some of these questions.

In the first study, we identified that the TB method calculated higher volumetric and lower EF and muscle mass values by comparing it to the CC technique in different hypertrabeculated populations while the 70% and 50% TB setups differed only in TPMi values. Considering the clinical impacts, the use of the TB method influenced the diagnostic and therapeutic decisions in all the studied CMP groups and healthy athletes. Thus, the TB method might be a useful tool in excessively trabeculated individuals, especially when interpreting borderline cases. However, updated normal values and criteria may be required for its broader application.

Our second study focused on the genetic background of symptomatic hypertrabeculated individuals with preserved LVEF, identifying pathogenic mutations in 25% of the population. Although LVNC individuals showed increased volumetric and muscle mass and decreased EF values compared to controls, no significant differences were reported among the LVNC genetic subgroups. Despite the similar CMR phenotypes, LVNC individuals with genetic mutations exhibited different clinical manifestations, namely a higher number of red flags than those without genetic involvement.

Our third study described reduced apical rotation and net cardiac twist in symptomatic hypertrabeculated individuals with preserved LVEF compared to controls, whereas cardiac rotational degrees were comparable among the LVNC genetic subgroups. In contrast, analyzing rotational patterns revealed differences among genotypes, as negative RBR was identified in a significant proportion of LVNC subjects carrying pathogenic or VUS mutations, whereas LVNC subjects from the B subgroup and control individuals showed only normal rotation or positive RBR. Additionally, the intermodality comparison of CMR-FT and Echo-ST methods described different degrees and consistent direction and pattern measurements.

7. Summary

Novel guidelines and recommendations differentiate hypertrabeculated phenotype in healthy individuals from hypertrabeculation with features of CMP (10, 16). Although the clinical spectrum of excessive trabeculation spans a wide range between the two abovementioned entities, diagnosing and managing the grey zone, namely symptomatic LVNC with preserved LVEF, remains challenging. These subjects require risk stratification to identify those at higher risk for further complications. Literature data suggests that advanced imaging techniques, identification of etiology, or genetic testing might be helpful. However, no proper risk stratification algorithm exists for LVNC with preserved LVEF (10, 16).

Our first study investigated the potential role of the TB method in the evaluation of different hypertrabeculated conditions. Although the TB technique is not yet a standard in routine clinical practice, our findings highlight its potential value, especially in borderline cases. Current normal values based on the CC technique are not directly applicable to the TB method, necessitating the development of modified criteria. The choice between the two methods can significantly impact diagnosis, risk assessment, and therapeutic decisions in hypertrabeculated individuals. However, using both methods as complementary tools could enhance the accuracy and quality of clinical decision-making.

Our second study identified that a high proportion of symptomatic LVNC individuals with preserved LVEF is genetically determined. We also highlighted that despite the comparable hypertrabeculated phenotype on the CMR images, the genetic and clinical background of LVNC is broad. As recent guidelines emphasize the role of underlying etiology and clinical symptoms in excessive trabeculation, our findings support the utility of a red flag system augmenting risk stratification and medical management.

Our third study analyzed the cardiac rotation in symptomatic excessive trabeculated subjects with preserved LVEF. We concluded that the reduction in apical rotation, which resulted in negative RBR, may stem from mechanical alterations caused by excessive trabeculation, particularly in LVNC with genetic involvement. Consequently, cardiac rotation could serve as an early marker of declining cardiac function and a potential warning sign during clinical follow-up of LVNC individuals with preserved LVEF.

8. References

1. Bentatou Z, Finas M, Habert P, Kober F, Guye M, Bricq S, et al. Distribution of left ventricular trabeculation across age and gender in 140 healthy Caucasian subjects on MR imaging. 2018(2211-5684 (Electronic)).
2. Meyer HV, Dawes TJW, Serrani M, Bai W, Tokarczuk P, Cai J, et al. Genetic and functional insights into the fractal structure of the heart.
3. Paun B, Bijnens B, Butakoff C. Relationship between the left ventricular size and the amount of trabeculations. Int J Numer Method Biomed Eng. 2018;34(3).
4. Choquet C, Nguyen THM, Sicard P, Buttigieg E, Tran TT, Kober F, et al. Deletion of Nkx2-5 in trabecular myocardium reveals the developmental origins of pathological heterogeneity associated with ventricular non-compaction cardiomyopathy. PLoS Genet. 2018;14(7):e1007502.
5. Freedom RM, Yoo S-J, Perrin D, Taylor G, Petersen S, Anderson RH. The morphological spectrum of ventricular noncompaction.
6. Oechslin E, Jenni R. Left ventricular non-compaction revisited: a distinct phenotype with genetic heterogeneity? Eur Heart J. 2011;32(12):1446-56.
7. Faber JW, D'Silva A, Christoffels VM, Jensen B. Lack of morphometric evidence for ventricular compaction in humans. J Cardiol. 2021;78(5):397-405.
8. Faber JW, Hagoort J, Moorman AFM, Christoffels VM, Jensen B. Quantified growth of the human embryonic heart. Biol Open. 2021;10(2).
9. Tian X, Li Y, He L, Zhang H, Huang X, Liu Q, et al. Identification of a hybrid myocardial zone in the mammalian heart after birth. Nat Commun. 2017;8(1):87.
10. Petersen SE, Jensen B, Aung N, Friedrich MG, McMahon CJ, Mohiddin SA, et al. Excessive Trabeculation of the Left Ventricle: JACC: Cardiovascular Imaging Expert Panel Paper. JACC Cardiovasc Imaging. 2023;16(3):408-25.
11. Kawel N, Nacif M, Arai AE, Gomes AS, Hundley WG, Johnson WC, et al. Trabeculated (noncompacted) and compact myocardium in adults: the multi-ethnic study of atherosclerosis. Circ Cardiovasc Imaging. 2012;5(3):357-66.
12. Gregor Z, Kiss AR, Szabó LE, Tóth A, Grebur K, Horváth M, et al. Sex- and age-specific normal values of left ventricular functional and myocardial mass parameters using threshold-based trabeculae quantification. PLoS One. 2021;16(10):e0258362.

13. Kawel-Boehm N, Hetzel SJ, Ambale-Venkatesh B, Captur G, Francois CJ, Jerosch-Herold M, et al. Reference ranges (“normal values”) for cardiovascular magnetic resonance (CMR) in adults and children: 2020 update.

14. Gati S, Chandra N, Bennett RL, Reed M, Kervio G, Panoulas VF, et al. Increased left ventricular trabeculation in highly trained athletes: do we need more stringent criteria for the diagnosis of left ventricular non-compaction in athletes? Heart. 2013;99(6):401-8.

15. Gati S, Papadakis M, Papamichael ND, Zaidi A, Sheikh N, Reed M, et al. Reversible de novo left ventricular trabeculations in pregnant women: implications for the diagnosis of left ventricular noncompaction in low-risk populations. Circulation. 2014;130(6):475-83.

16. Arbelo E, Protonotarios A, Gimeno JR, Arbustini E, Barriales-Villa R, Basso C, et al. 2023 ESC Guidelines for the management of cardiomyopathies. Eur Heart J. 2023.

17. Zemrak F, Ahlman MA, Captur G, Mohiddin SA, Kawel-Boehm N, Prince MR, et al. The relationship of left ventricular trabeculation to ventricular function and structure over a 9.5-year follow-up: the MESA study. J Am Coll Cardiol. 2014;64(19):1971-80.

18. Weir-McCall JR, Yeap PM, Papagiorcopulo C, Fitzgerald K, Gandy SJ, Lambert M, et al. Left Ventricular Noncompaction: Anatomical Phenotype or Distinct Cardiomyopathy? J Am Coll Cardiol. 2016;68(20):2157-65.

19. Abela M, D'Silva A. Left Ventricular Trabeculations in Athletes: Epiphenomenon or Phenotype of Disease? Curr Treat Options Cardiovasc Med. 2018;20(12):100.

20. Pelliccia A, Sharma S, Gati S, Bäck M, Börjesson M, Caselli S, et al. 2020 ESC Guidelines on Sports Cardiology and Exercise in Patients with Cardiovascular Disease. Rev Esp Cardiol (Engl Ed). 2021;74(6):545.

21. Czimbalmos C, Csecs I, Toth A, Kiss O, Suhai FI, Sydo N, et al. The demanding grey zone: Sport indices by cardiac magnetic resonance imaging differentiate hypertrophic cardiomyopathy from athlete’s heart. PLoS One. 2019;14(2):e0211624.

22. Pelliccia A, Solberg EE, Papadakis M, Adami PE, Biffi A, Caselli S, et al. Recommendations for participation in competitive and leisure time sport in athletes with cardiomyopathies, myocarditis, and pericarditis: position statement of the Sport Cardiology Section of the European Association of Preventive Cardiology (EAPC). Eur Heart J. 2019;40(1):19-33.

23. Petek BJ, Groezinger EY, Pedlar CR, Baggish AL. Cardiac effects of detraining in athletes: A narrative review. Ann Phys Rehabil Med. 2022;65(4):101581.
24. Jagminas R, Šerpytis R, Šerpytis P, Glaveckaitė S. Left Ventricular Hypertrabeculation (LVHT) in Athletes: A Negligible Finding? Medicina (Kaunas). 61. Switzerland2024.
25. Pelliccia A, Sharma S, Gati S, Bäck M, Börjesson M, Caselli S, et al. 2020 ESC Guidelines on sports cardiology and exercise in patients with cardiovascular disease. Eur Heart J. 2021;42(1):17-96.
26. Stähli BE, Gebhard C, Biaggi P, Klaassen S, Valsangiacomo Buechel E, Attenhofer Jost CH, et al. Left ventricular non-compaction: prevalence in congenital heart disease. Int J Cardiol. 2013;167(6):2477-81.
27. Tian T, Yang Y, Zhou L, Luo F, Li Y, Fan P, et al. Left Ventricular Non-Compaction: A Cardiomyopathy With Acceptable Prognosis in Children. Heart Lung Circ. 2018;27(1):28-32.
28. Mazzarotto F, Hawley MH, Beltrami M, Beekman L, de Marvao A, McGurk KA, et al. Systematic large-scale assessment of the genetic architecture of left ventricular noncompaction reveals diverse etiologies. Genetics in Medicine. 2021;23(5):856-64.
29. Marcus FI, McKenna WJ, Sherrill D, Basso C, Bauce B, Bluemke DA, et al. Diagnosis of arrhythmogenic right ventricular cardiomyopathy/dysplasia: proposed modification of the Task Force Criteria. Eur Heart J. 2010;31(7):806-14.
30. Corrado D, Basso C, Rizzoli G, Schiavon M, Thiene G. Does sports activity enhance the risk of sudden death in adolescents and young adults? J Am Coll Cardiol. 2003;42(11):1959-63.
31. Peterson DF, Kucera K, Thomas LC, Maleszewski J, Siebert D, Lopez-Anderson M, et al. Aetiology and incidence of sudden cardiac arrest and death in young competitive athletes in the USA: a 4-year prospective study. Br J Sports Med. 2021;55(21):1196-203.
32. Gerecke BJ, Engberding R. Noncompaction Cardiomyopathy-History and Current Knowledge for Clinical Practice. J Clin Med. 2021;10(11).
33. Lorca R, Martín M, Pascual I, Astudillo A, Díaz Molina B, Cigarrán H, et al. Characterization of Left Ventricular Non-Compaction Cardiomyopathy. J Clin Med. 2020;9(8).

34. Ichida F. Left ventricular noncompaction - Risk stratification and genetic consideration. J Cardiol. 2020;75(1):1-9.
35. Piekutowska-Abramczuk D, Paszkowska A, Ciara E, Frączak K, Mirecka-Rola A, Wicher D, et al. Genetic Profile of Left Ventricular Noncompaction Cardiomyopathy in Children-A Single Reference Center Experience. Genes (Basel). 2022;13(8).
36. Liu S, Xie Y, Zhang H, Feng Z, Huang J, Hu S, et al. Multiple genetic variants in adolescent patients with left ventricular noncompaction cardiomyopathy. International Journal of Cardiology. 2020;302:117-23.
37. van Waning JI, Caliskan K, Hoedemaekers YM, van Spaendonck-Zwarts KY, Baas AF, Boekholdt SM, et al. Genetics, Clinical Features, and Long-Term Outcome of Noncompaction Cardiomyopathy. J Am Coll Cardiol. 2018;71(7):711-22.
38. Li S, Zhang C, Liu N, Bai H, Hou C, Wang J, et al. Genotype-Positive Status Is Associated With Poor Prognoses in Patients With Left Ventricular Noncompaction Cardiomyopathy. J Am Heart Assoc. 2018;7(20):e009910.
39. Takasaki A, Hirono K, Hata Y, Wang C, Takeda M, Yamashita JK, et al. Sarcomere gene variants act as a genetic trigger underlying the development of left ventricular noncompaction. Pediatr Res. 2018;84(5):733-42.
40. Liu Y, Chen HY, Shou WN. Potential Common Pathogenic Pathways for the Left Ventricular Noncompaction Cardiomyopathy (LVNC). Pediatric Cardiology. 2018;39(6):1099-106.
41. Chimenti C, Lavalle C, Magnocavallo M, Alfarano M, Mariani MV, Bernardini F, et al. A proposed strategy for anticoagulation therapy in noncompaction cardiomyopathy. Esc Heart Failure. 2022;9(1):241-50.
42. Miyake CY, Kim JJ. Arrhythmias in left ventricular noncompaction. Card Electrophysiol Clin. 2015;7(2):319-30.
43. Vergani V, Lazzeroni D, Peretto G. Bridging the gap between hypertrabeculation phenotype, noncompaction phenotype and left ventricular noncompaction cardiomyopathy. J Cardiovasc Med (Hagerstown). 2020;21(3):192-9.
44. Negri F, De Luca A, Fabris E, Korcova R, Cernetti C, Grigoratos C, et al. Left ventricular noncompaction, morphological, and clinical features for an integrated diagnosis. Heart Fail Rev. 2019;24(3):315-23.

45. Grebur K, Mester B, Fekete BA, Kiss AR, Gregor Z, Horváth M, et al. Genetic, clinical and imaging implications of a noncompaction phenotype population with preserved ejection fraction. Front Cardiovasc Med. 2024;11:1337378.
46. Chin TK, Perloff JK, Williams RG, Jue K, Mohrmann R. Isolated noncompaction of left ventricular myocardium. A study of eight cases. Circulation. 1990;82(2):507-13.
47. Jenni R, Oechslin E, Schneider J, Attenhofer Jost C, Kaufmann PA. Echocardiographic and pathoanatomical characteristics of isolated left ventricular non-compaction: a step towards classification as a distinct cardiomyopathy. Heart. 2001;86(6):666-71.
48. Stollberger C, Streit N, Yoshida T, Wegner C, Finsterer J. Left ventricular hypertrabeculation/noncompaction and pregnancy. International Journal of Cardiology. 2014;172(1):271-3.
49. de Groot-de Laat LE, Krenning BJ, ten Cate FJ, Roelandt JR. Usefulness of contrast echocardiography for diagnosis of left ventricular noncompaction. Am J Cardiol. 2005;95(9):1131-4.
50. Captur G, Syrris P, Obianyo C, Limongelli G, Moon JC. Formation and Malformation of Cardiac Trabeculae: Biological Basis, Clinical Significance, and Special Yield of Magnetic Resonance Imaging in Assessment. Can J Cardiol. 2015;31(11):1325-37.
51. Weinsaft JW, Cham MD, Janik M, Min JK, Henschke CI, Yankelevitz DF, et al. Left ventricular papillary muscles and trabeculae are significant determinants of cardiac MRI volumetric measurements: effects on clinical standards in patients with advanced systolic dysfunction. Int J Cardiol. 2008;126(3):359-65.
52. Jacquier A, Thuny F, Jop B, Giorgi R, Cohen F, Gaubert JY, et al. Measurement of trabeculated left ventricular mass using cardiac magnetic resonance imaging in the diagnosis of left ventricular non-compaction. Eur Heart J. 2010;31(9):1098-104.
53. Grothoff M, Pachowsky M, Hoffmann J, Posch M, Klaassen S, Lehmkuhl L, et al. Value of cardiovascular MR in diagnosing left ventricular non-compaction cardiomyopathy and in discriminating between other cardiomyopathies. Eur Radiol. 2012;22(12):2699-709.

54. Stacey RB, Andersen MM, St Clair M, Hundley WG, Thohan V. Comparison of systolic and diastolic criteria for isolated LV noncompaction in CMR. JACC Cardiovasc Imaging. 2013;6(9):931-40.

55. Schulz-Menger J, Bluemke DA, Bremerich J, Flamm SD, Fogel MA, Friedrich MG, et al. Standardized image interpretation and post-processing in cardiovascular magnetic resonance - 2020 update : Society for Cardiovascular Magnetic Resonance (SCMR): Board of Trustees Task Force on Standardized Post-Processing. J Cardiovasc Magn Reson. 2020;22(1):19.

56. Jaspers K, Freling HG, van Wijk K, Romijn EI, Greuter MJ, Willems TP. Improving the reproducibility of MR-derived left ventricular volume and function measurements with a semi-automatic threshold-based segmentation algorithm. Int J Cardiovasc Imaging. 2013;29(3):617-23.

57. Csecs I, Czimbalmos C, Suhai FI, Mikle R, Mirzahosseini A, Dohy Z, et al. Left and right ventricular parameters corrected with threshold-based quantification method in a normal cohort analyzed by three independent observers with various training-degree. Int J Cardiovasc Imaging. 2018;34(7):1127-33.

58. Hautvast G, Breeuwer M, Lobregt S, Gerritsen F. Automatic exclusion of papillary muscles and trabeculae from blood volume measurements in cine cardiac magnetic resonance images.

59. Varga-Szemes A, Muscogiuri G, Schoepf UJ, Wichmann JL, Suranyi P, De Cecco CN, et al. Clinical feasibility of a myocardial signal intensity threshold-based semi-automated cardiac magnetic resonance segmentation method. European Radiology. 2016;26(5):1503-11.

60. Andreini D, Pontone G, Bogaert J, Roghi A, Barison A, Schwitter J, et al. Long-Term Prognostic Value of Cardiac Magnetic Resonance in Left Ventricle Noncompaction: A Prospective Multicenter Study. J Am Coll Cardiol. 2016;68(20):2166-81.

61. Grigoratos C, Barison A, Ivanov A, Andreini D, Amzulescu MS, Mazurkiewicz L, et al. Meta-Analysis of the Prognostic Role of Late Gadolinium Enhancement and Global Systolic Impairment in Left Ventricular Noncompaction. JACC Cardiovasc Imaging. 2019;12(11 Pt 1):2141-51.

62. Kayvanpour E, Sedaghat-Hamedani F, Gi WT, Tugrul OF, Amr A, Haas J, et al. Clinical and genetic insights into non-compaction: a meta-analysis and systematic review on 7598 individuals. Clin Res Cardiol. 2019;108(11):1297-308.

63. Grebur K, Gregor Z, Kiss AR, Horváth M, Mester B, Czimbalmos C, et al. Different methods, different results? Threshold-based versus conventional contouring techniques in clinical practice. Int J Cardiol. 2023.

64. Schuster A, Hor KN, Kowallick JT, Beerbaum P, Kutty S. Cardiovascular Magnetic Resonance Myocardial Feature Tracking: Concepts and Clinical Applications. Circ Cardiovasc Imaging. 2016;9(4):e004077.

65. Sengupta PP, Tajik AJ, Chandrasekaran K, Khandheria BK. Twist mechanics of the left ventricle: principles and application. JACC Cardiovasc Imaging. 2008;1(3):366-76.

66. Anwer S, Heiniger PS, Rogler S, Erhart L, Cassani D, Kuzo N, et al. Left ventricular mechanics and cardiovascular outcomes in non-compaction phenotype. Int J Cardiol. 2021;336:73-80.

67. Kiss AR, Gregor Z, Furak A, Tóth A, Horváth M, Szabo L, et al. Left ventricular characteristics of noncompaction phenotype patients with good ejection fraction measured with cardiac magnetic resonance. Anatol J Cardiol. 2021;25(8):565-71.

68. Gregor Z, Kiss AR, Grebur K, Szabó LE, Merkely B, Vágó H, et al. MR -specific characteristics of left ventricular noncompaction and dilated cardiomyopathy. Int J Cardiol. 2022;359:69-75.

69. Voigt JU, Pedrizzetti G, Lysyansky P, Marwick TH, Houle H, Baumann R, et al. Definitions for a common standard for 2D speckle tracking echocardiography: consensus document of the EACVI/ASE/Industry Task Force to standardize deformation imaging. Eur Heart J Cardiovasc Imaging. 2015;16(1):1-11.

70. Nemes A, Kormányos Á. Prevalence of left ventricular 'rigid body rotation', the near absence of left ventricular twist (insights from the MAGYAR studies). Rev Cardiovasc Med. 2022;23(1):5.

71. Grebur K, Mester B, Horváth M, Farkas-Sütő K, Gregor Z, Kiss AR, et al. The effect of excessive trabeculation on cardiac rotation-A multimodal imaging study. PLoS One. 2024;19(9):e0308035.

72. Notomi Y, Srinath G, Shiota T, Martin-Miklovic MG, Beachler L, Howell K, et al. Maturational and adaptive modulation of left ventricular torsional biomechanics: Doppler tissue imaging observation from infancy to adulthood. Circulation. 2006;113(21):2534-41.

73. Szűcs A, Kiss AR, Gregor Z, Horváth M, Tóth A, Dohy Z, et al. Changes in strain parameters at different deterioration levels of left ventricular function: A cardiac magnetic resonance feature-tracking study of patients with left ventricular noncompaction. Int J Cardiol. 2021;331:124-30.

74. Popescu BA, Beladan CC, Calin A, Muraru D, Deleanu D, Rosca M, et al. Left ventricular remodelling and torsional dynamics in dilated cardiomyopathy: reversed apical rotation as a marker of disease severity. Eur J Heart Fail. 2009;11(10):945-51.

75. Maharaj N, Khandheria BK, Peters F, Libhaber E, Essop MR. Time to twist: marker of systolic dysfunction in Africans with hypertension. Eur Heart J Cardiovasc Imaging. 2013;14(4):358-65.

76. Peters F, Khandheria BK, Libhaber E, Maharaj N, Dos Santos C, Matioda H, et al. Left ventricular twist in left ventricular noncompaction. Eur Heart J Cardiovasc Imaging. 2014;15(1):48-55.

77. van Dalen BM, Caliskan K, Soliman OI, Nemes A, Vletter WB, Ten Cate FJ, et al. Left ventricular solid body rotation in non-compaction cardiomyopathy: a potential new objective and quantitative functional diagnostic criterion? Eur J Heart Fail. 2008;10(11):1088-93.

78. van Dalen BM, Caliskan K, Soliman OI, Kauer F, van der Zwaan HB, Vletter WB, et al. Diagnostic value of rigid body rotation in noncompaction cardiomyopathy. J Am Soc Echocardiogr. 2011;24(5):548-55.

79. Guigui SA, Horvath SA, Arenas IA, Mihos CG. Cardiac geometry, function and mechanics in left ventricular non-compaction cardiomyopathy with preserved ejection fraction. J Echocardiogr. 2022;20(3):144-50.

80. Nawaytou HM, Montero AE, Yubbu P, Calderón-Anyosa RJC, Sato T, O'Connor MJ, et al. A Preliminary Study of Left Ventricular Rotational Mechanics in Children with Noncompaction Cardiomyopathy: Do They Influence Ventricular Function? J Am Soc Echocardiogr. 2018;31(8):951-61.

81. Richards S, Aziz N, Bale S, Bick D, Das S, Gastier-Foster J, et al. Standards and guidelines for the interpretation of sequence variants: a joint consensus recommendation of the American College of Medical Genetics and Genomics and the Association for Molecular Pathology. Genet Med. 2015;17(5):405-24.

82. van Waning JI, Caliskan K, Chelu RG, van der Velde N, Pezzato A, Michels M, et al. Diagnostic Cardiovascular Magnetic Resonance Imaging Criteria in Noncompaction Cardiomyopathy and the Yield of Genetic Testing. Canadian Journal of Cardiology. 2021;37(3):433-42.

83. Elliott P, Andersson B, Arbustini E, Bilinska Z, Cecchi F, Charron P, et al. Classification of the cardiomyopathies: a position statement from the European Society Of Cardiology Working Group on Myocardial and Pericardial Diseases. Eur Heart J. 2008;29(2):270-6.

84. Petersen SE, Selvanayagam JB, Wiesmann F, Robson MD, Francis JM, Anderson RH, et al. Left ventricular non-compaction: insights from cardiovascular magnetic resonance imaging. J Am Coll Cardiol. 2005;46(1):101-5.

85. Szűcs A, Kiss AR, Suhai FI, Tóth A, Gregor Z, Horváth M, et al. The effect of contrast agents on left ventricular parameters calculated by a threshold-based software module: does it truly matter? Int J Cardiovasc Imaging. 2019;35(9):1683-9.

86. De Lazzari M, Brunetti G, Frasson E, Zorzi A, Cipriani A, Migliore F, et al. Thinning of compact layer and systolic dysfunction in isolated left ventricular non-compaction: A cardiac magnetic resonance study. Int J Cardiol. 2024;397:131614.

87. Hor KN, Baumann R, Pedrizzetti G, Tonti G, Gottliebson WM, Taylor M, et al. Magnetic resonance derived myocardial strain assessment using feature tracking. J Vis Exp. 2011(48).

88. Alfakih K, Plein S, Thiele H, Jones T, Ridgway JP, Sivananthan MU. Normal human left and right ventricular dimensions for MRI as assessed by turbo gradient echo and steady-state free precession imaging sequences. J Magn Reson Imaging. 2003;17(3):323-9.

89. Csecs I, Czimbalmos C, Toth A, Dohy Z, Suhai IF, Szabo L, et al. The impact of sex, age and training on biventricular cardiac adaptation in healthy adult and adolescent athletes: Cardiac magnetic resonance imaging study. Eur J Prev Cardiol. 2020;27(5):540-9.

90. Goffinet C, Chenot F, Robert A, Pouleur AC, le Polain de Waroux JB, Vancrayenest D, et al. Assessment of subendocardial vs. subepicardial left ventricular rotation and twist using two-dimensional speckle tracking echocardiography: comparison with tagged cardiac magnetic resonance. Eur Heart J. 2009;30(5):608-17.

91. Ashwal AJ, Mugula SR, Samanth J, Paramasivam G, Nayak K, Padmakumar R. Role of deformation imaging in left ventricular non-compaction and hypertrophic cardiomyopathy: an Indian perspective. Egypt Heart J. 2020;72(1):6.

92. Arbustini E, Weidemann F, Hall JL. Left ventricular noncompaction: a distinct cardiomyopathy or a trait shared by different cardiac diseases? J Am Coll Cardiol. 2014;64(17):1840-50.

93. McDonagh TA, Metra M, Adamo M, Gardner RS, Baumbach A, Böhm M, et al. 2021 ESC Guidelines for the diagnosis and treatment of acute and chronic heart failure. Eur Heart J. 2021;42(36):3599-726.

94. Towbin JA, McKenna WJ, Abrams DJ, Ackerman MJ, Calkins H, Darrieux FCC, et al. 2019 HRS expert consensus statement on evaluation, risk stratification, and management of arrhythmogenic cardiomyopathy. Heart Rhythm. 2019;16(11):e301-e72.

95. Mitropoulou P, Georgiopoulos G, Figliozzi S, Klettas D, Nicoli F, Masci PG. Multi-Modality Imaging in Dilated Cardiomyopathy: With a Focus on the Role of Cardiac Magnetic Resonance. Front Cardiovasc Med. 2020;7:97.

96. Murphy RT, Thaman R, Blanes JG, Ward D, Sevdalis E, Papra E, et al. Natural history and familial characteristics of isolated left ventricular non-compaction. Eur Heart J. 2005;26(2):187-92.

97. Frandon J, Bricq S, Bentatou Z, Marcadet L, Barral PA, Finas M, et al. Semi-automatic detection of myocardial trabeculation using cardiovascular magnetic resonance: correlation with histology and reproducibility in a mouse model of non-compaction.

98. Quick S, Waessnig N, Sommer P, Heidrich FM, Pfluecke C, Ibrahim K, et al. Impact of papillary muscles on ventricular function measurements in 3T cardiac magnetic resonance. Cor et Vasa. 2017;59(2):e142-e8.

99. Riffel JH, Schmucker K, Andre F, Ochs M, Hirschberg K, Schaub E, et al. Cardiovascular magnetic resonance of cardiac morphology and function: impact of

different strategies of contour drawing and indexing. Clin Res Cardiol. 2019;108(4):411-29.

100. Kim HJ, Mun DN, Goo HW, Yun TJ. Use of Cardiac Computed Tomography for Ventricular Volumetry in Late Postoperative Patients with Tetralogy of Fallot. Korean J Thorac Cardiovasc Surg. 2017;50(2):71-7.

101. Stöllberger C, Blazek G, Dobias C, Hanafin A, Wegner C, Finsterer J. Frequency of stroke and embolism in left ventricular hypertrabeculation/noncompaction. Am J Cardiol. 2011;108(7):1021-3.

102. Kiss AR, Gregor Z, Popovics A, Grebur K, Szabó LE, Dohy Z, et al. Impact of Right Ventricular Trabeculation on Right Ventricular Function in Patients With Left Ventricular Non-compaction Phenotype. Front Cardiovasc Med. 2022;9:843952.

103. Miszalski-Jamka K, Jefferies JL, Mazur W, Głowacki J, Hu J, Lazar M, et al. Novel Genetic Triggers and Genotype-Phenotype Correlations in Patients With Left Ventricular Noncompaction. Circ Cardiovasc Genet. 2017;10(4).

104. Ivanov A, Dabiesingh DS, Bhumireddy GP, Mohamed A, Asfour A, Briggs WM, et al. Prevalence and Prognostic Significance of Left Ventricular Noncompaction in Patients Referred for Cardiac Magnetic Resonance Imaging. Circ Cardiovasc Imaging. 2017;10(9).

105. Richard P, Ader F, Roux M, Donal E, Eicher JC, Aoutil N, et al. Targeted panel sequencing in adult patients with left ventricular non-compaction reveals a large genetic heterogeneity. Clin Genet. 2019;95(3):356-67.

106. Vershinina T, Fomicheva Y, Muravyev A, Jorholt J, Kozyreva A, Kiselev A, et al. Genetic Spectrum of Left Ventricular Non-Compaction in Paediatric Patients. Cardiology (Switzerland). 2020;145(11):746-55.

107. Hoedemaekers YM, Caliskan K, Michels M, Frohn-Mulder I, van der Smagt JJ, Phefferkorn JE, et al. The Importance of Genetic Counseling, DNA Diagnostics, and Cardiologic Family Screening in Left Ventricular Noncompaction Cardiomyopathy. Circulation-Cardiovascular Genetics. 2010;3(3):232-U43.

108. Steffel J, Kobza R, Oechslin E, Jenni R, Duru F. Electrocardiographic characteristics at initial diagnosis in patients with isolated left ventricular noncompaction. Am J Cardiol. 2009;104(7):984-9.

109. Brescia ST, Rossano JW, Pignatelli R, Jefferies JL, Price JF, Decker JA, et al. Mortality and sudden death in pediatric left ventricular noncompaction in a tertiary referral center. Circulation. 2013;127(22):2202-8.

110. Balla C, De Raffele M, Deserio MA, Sanchini M, Farnè M, Trabanelli C, et al. Left Ventricular Myocardial Noncompaction with Advanced Atrioventricular Conduction Disorder and Ventricular Arrhythmias in a Young Patient: Role of MIB1 Gene. J Cardiovasc Dev Dis. 8. Switzerland2021.

111. Wilde AAM, Semsarian C, Márquez MF, Shamloo AS, Ackerman MJ, Ashley EA, et al. European Heart Rhythm Association (EHRA)/Heart Rhythm Society (HRS)/Asia Pacific Heart Rhythm Society (APHRS)/Latin American Heart Rhythm Society (LAHRS) Expert Consensus Statement on the state of genetic testing for cardiac diseases. Europace. 2022;24(8):1307-67.

112. Gastl M, Gotschy A, Polacin M, Vishnevskiy V, Meyer D, Sokolska J, et al. Determinants of myocardial function characterized by CMR-derived strain parameters in left ventricular non-compaction cardiomyopathy. Sci Rep. 2019;9(1):15882.

113. Akhan O, Demir E, Dogdus M, Cakan FO, Nalbantgil S. Speckle tracking echocardiography and left ventricular twist mechanics: predictive capabilities for noncompaction cardiomyopathy in the first degree relatives. Int J Cardiovasc Imaging. 2021;37(2):429-38.

114. Sabatino J, Di Salvo G, Krupickova S, Fraisse A, Prota C, Bucciarelli V, et al. Left Ventricular Twist Mechanics to Identify Left Ventricular Noncompaction in Childhood. Circ Cardiovasc Imaging. 2019;12(4):e007805.

115. Kanzaki H, Nakatani S, Yamada N, Urayama S, Miyatake K, Kitakaze M. Impaired systolic torsion in dilated cardiomyopathy: reversal of apical rotation at mid-systole characterized with magnetic resonance tagging method. Basic Res Cardiol. 2006;101(6):465-70.

116. Beaumont A, Grace F, Richards J, Hough J, Oxborough D, Sculthorpe N. Left Ventricular Speckle Tracking-Derived Cardiac Strain and Cardiac Twist Mechanics in Athletes: A Systematic Review and Meta-Analysis of Controlled Studies. Sports Med. 2017;47(6):1145-70.

117. Kim WJ, Lee BH, Kim YJ, Kang JH, Jung YJ, Song JM, et al. Apical rotation assessed by speckle-tracking echocardiography as an index of global left ventricular contractility. Circ Cardiovasc Imaging. 2009;2(2):123-31.

118. Kormányos Á, Kalapos A, Domsik P, Lengyel C, Forster T, Nemes A. Normal values of left ventricular rotational parameters in healthy adults-Insights from the three-dimensional speckle tracking echocardiographic MAGYAR-Healthy Study. Echocardiography. 2019;36(4):714-21.

119. Taylor RJ, Umar F, Lin EL, Ahmed A, Moody WE, Mazur W, et al. Mechanical effects of left ventricular midwall fibrosis in non-ischemic cardiomyopathy. J Cardiovasc Magn Reson. 2016;18:1.

120. Augustine D, Lewandowski AJ, Lazdam M, Rai A, Francis J, Myerson S, et al. Global and regional left ventricular myocardial deformation measures by magnetic resonance feature tracking in healthy volunteers: comparison with tagging and relevance of gender. J Cardiovasc Magn Reson. 2013;15(1):8.

121. Obokata M, Nagata Y, Wu VC, Kado Y, Kurabayashi M, Otsuji Y, et al. Direct comparison of cardiac magnetic resonance feature tracking and 2D/3D echocardiography speckle tracking for evaluation of global left ventricular strain. Eur Heart J Cardiovasc Imaging. 2016;17(5):525-32.

122. Taha K, Bourfiss M, Te Riele A, Cramer MM, van der Heijden JF, Asselbergs FW, et al. A head-to-head comparison of speckle tracking echocardiography and feature tracking cardiovascular magnetic resonance imaging in right ventricular deformation. Eur Heart J Cardiovasc Imaging. 2021;22(8):950-8.

123. Manole S, Budurea C, Pop S, Iliescu AM, Ciortea CA, Iancu SD, et al. Correlation between Volumes Determined by Echocardiography and Cardiac MRI in Controls and Atrial Fibrillation Patients. Life (Basel). 2021;11(12).

9. Bibliography of the candidate's publications

9.1 Publications related to the PhD thesis

1. **Grebur K**, Gregor Z, Kiss AR, Horváth M, Mester B, Czimbalmos C, Tóth A, Szabó LE, Dohy Z, Vágó H, Merkely B, Szűcs A. Different methods, different results? Threshold-based versus conventional contouring techniques in clinical practice. Int J Cardiol. 2023 Jun 15;381:128-134. doi: 10.1016/j.ijcard.2023.03.051. Epub 2023 Mar 23. PMID: 36965638, IF: 3,2.

2. **Grebur K**, Mester B, Fekete BA, Kiss AR, Gregor Z, Horváth M, Farkas-Sütő K, Csonka K, Bödör C, Merkely B, Vágó H, Szűcs A. Genetic, clinical and imaging implications of a noncompaction phenotype population with preserved ejection fraction. Front Cardiovasc Med. 2024 Feb 6;11:1337378. doi: 10.3389/fcvm.2024.1337378. PMID: 38380180; PMCID: PMC10876896, IF: 2,8.

3. **Grebur K**, Mester B, Horváth M, Farkas-Sütő K, Gregor Z, Kiss AR, Tóth A, Kovács A, Fábián A, Lakatos BK, Fekete BA, Csonka K, Bödör C, Merkely B, Vágó H, Szűcs A. The effect of excessive trabeculation on cardiac rotation-A multimodal imaging study. PLoS One. 2024 Sep 5;19(9):e0308035. doi: 10.1371/journal.pone.0308035. PMID: 39236040; PMCID: PMC11376564, IF: 2,9.

9.2 Publications not related to the PhD thesis

1. Gregor Z, Kiss AR, Szabó LE, Tóth A, **Grebur K**, Horváth M, Dohy Z, Merkely B, Vágó H, Szűcs A. Sex- and age- specific normal values of left ventricular functional and myocardial mass parameters using threshold-based trabeculae quantification. PLoS One. 2021 Oct 12;16(10):e0258362. doi: 10.1371/journal.pone.0258362. PMID: 34637474; PMCID: PMC8509873., IF: 3,752

2. Gregor Z, Kiss AR, **Grebur K**, Szabó LE, Merkely B, Vágó H, Szűcs A. MR -specific characteristics of left ventricular noncompaction and dilated cardiomyopathy. Int J Cardiol. 2022 Jul 15;359:69-75. doi: 10.1016/j.ijcard.2022.04.026. Epub 2022 Apr 15. PMID: 35436556. , IF: 3,5

3. Kiss AR, Gregor Z, Popovics A, **Grebur K**, Szabó LE, Dohy Z, Kovács A, Lakatos BK, Merkely B, Vágó H, Szũcs A. Impact of Right Ventricular Trabeculation on Right Ventricular Function in Patients With Left Ventricular Non-compaction Phenotype. Front

Cardiovasc Med. 2022 Apr 12;9:843952. doi: 10.3389/fcvm.2022.843952. PMID: 35498016; PMCID: PMC9041027., IF: 3,6

4. Gregor Z, Kiss AR, **Grebur K**, Dohy Z, Kovács A, Merkely B, Vágó H, Szűcs A. Characteristics of the right ventricle in left ventricular noncompaction with reduced ejection fraction in the light of dilated cardiomyopathy. PLoS One. 2023 Sep 25;18(9):e0290981. doi: 10.1371/journal.pone.0290981. PMID: 37747903; PMCID: PMC10519585., IF: 2,9

5. Horváth M, Farkas-Sütő K, Fábián A, Lakatos B, Kiss AR, **Grebur K**, Gregor Z, Mester B, Kovács A, Merkely B, Szűcs A. Highlights of right ventricular characteristics of left ventricular noncompaction using 3D echocardiography. Int J Cardiol Heart Vasc. 2023 Nov 15;49:101289. doi: 10.1016/j.ijcha.2023.101289. PMID: 38035261; PMCID: PMC10684825. , IF: 2,5

6. Ujvári A, Fábián A, Lakatos B, Tokodi M, Ladányi Z, Sydó N, Csulak E, Vágó H, Juhász V, **Grebur K**, Szűcs A, Zámodics M, Babity M, Kiss O, Merkely B, Kovács A. Right Ventricular Structure and Function in Adolescent Athletes: A 3D Echocardiographic Study. Int J Sports Med. 2024 Jun;45(6):473-480. doi: 10.1055/a-2259-2203. Epub 2024 Feb 1. PMID: 38301728; PMCID: PMC11150038., IF: 2

7. Farkas-Sütő KA, **Grebur K**, Mester B, Gyulánczi FK, Bödör C, Vágó H, Merkely B, Szűcs A. Electrocardiogram Features of Left Ventricular Excessive Trabeculation with Preserved Cardiac Function in Light of Cardiac Magnetic Resonance and Genetics. J Clin Med. 2024 Oct 3;13(19):5906. doi: 10.3390/jcm13195906. PMID: 39407966; PMCID: PMC11477278., IF: 3,0

8. Mester B, Lipták Z, Farkas-Sütő KA, **Grebur K**, Gyulánczi FK, Fábián A, Fekete BA, György TA, Bödör C, Kovács A, Merkely B, Szűcs A. Inherited Hypertrabeculation? Genetic and Clinical Insights in Blood Relatives of Genetically Affected Left Ventricular Excessive Trabeculation Patients. Life (Basel). 2025 Jan 22;15(2):150. doi: 10.3390/life15020150. PMID: 40003559; PMCID: PMC11856360., IF: 3,2

9. Horváth M, Kiss D, Márkusz I, Tokodi M, Kiss AR, Gregor Z, **Grebur K**, Farkas-Sütő K, Mester B, Gyulánczi F, Kovács A, Merkely B, Vágó H, Szűcs A. Comparison of Imaging Modalities for Left Ventricular Noncompaction Morphology. J Imaging. 2025

Jun 4;11(6):185. doi: 10.3390/jimaging11060185. PMID: 40558784; PMCID: PMC12194762, IF: 3,3

10. Horváth M, Farkas-Sütő K, Gyulánczi FK, Fábián A, Lakatos B, Kiss AR, **Grebur K**, Gregor Z, Mester B, Kovács A, Merkely B, Szűcs A. 3D Echocardiographic Assessment of Right Ventricular Involvement of Left Ventricular Hypertrabecularization from a New Perspective. J Imaging. 2025 Jun 3;11(6):181. doi: 10.3390/jimaging11060181. PMID: 40558780; PMCID: PMC12194596, IF: 3,3

11. Zamodics M, Babity M, Schay G, Bucsko-Varga A, Kovacs E, Horvath M, **Grebur K**, Laszlo MJ, Fabian A, Lakatos BK, Herczeg S, Vago H, Kovacs A, Merkely B, Kiss O. Investigation of Body Composition and Cardiac Sports Adaptation in Elite Water Polo Players. Sports (Basel). 2025 Jun 9;13(6):180. doi: 10.3390/sports13060180. PMID: 40559692; PMCID: PMC12196840, IF: 2,9

12. Mester B, Farkas-Sütő KA, Tardy JM, **Grebur K**, Horváth M, Gyulánczi FK, Vágó H, Merkely B, Szűcs A. New Solution for Segmental Assessment of Left Ventricular Wall Thickness, Using Anatomically Accurate and Highly Reproducible Automated Cardiac MRI Software. J Imaging. 2025 Oct 11;11(10):357. doi: 10.3390/jimaging11100357. PMID: 41150033; PMCID: PMC12565150, IF: 3,3

10. Acknowledgements

I would like to express my deepest gratitude to everyone who has contributed to the completion of my PhD degree.

I would like to thank to Prof.Dr. Merkely Béla, the rector of the Semmelweis University, for providing me with the opportunity to pursue my PhD, as well as for the scientific and financial support that made this research possible.

I would like to express my deepest appreciation to my supervisor, Dr. Szűcs Andrea, whose endless help, patience and guidance have profoundly shaped my development — not only in research but also in clinical practice and personal life.

I am also thankful to Dr.Kiss Anna Réka, Dr.Gregor Zsófia and Dr.Horváth Márton, who firstly were my mentors and later became my colleagues, supporting me in scientific and personal life. I would like to thank Dr.Mester Balázs and Dr. Farkas-Sütő Kristóf, who started as my TDK students and later continued my noncompaction research, I cherish the great moments we shared.

My gratitude extends to the CMR team, especially Dr.Vágó Hajnalka, Dr.Tóth Attila, Dr. Szabó Liliána Erzsébet and Dr. Dohy Zsófia for their knowledge and helpful advices regarding my research projects; as well as to the echocardiography team, especially Dr.Kovács Attila, Dr. Lakatos Bálint, Dr.Fábián Alexandra and Dr.Ladányi Zsuzsanna, for guiding me in the scientific interpretation of echocardiographic examinations. Additionally, I appreciate the Department of Pathology and Experimental Cancer Research Department, especially Dr.Bödör Csaba, Dr.Fekete Bálint András and Dr.Csonka Katalin, for their guidance in analyzing and interpreting genetic data. I would also like to acknowledge all the scientific research students and assistants, who contributed to these projects.

I would like to thank to my „PhD friends", who helped to navigate the administrative aspects of the PhD process, I am grateful for the teamwork and shared efforts. Special thanks go to „ELTE Márton Áron Szakkollégium", which started to support my research as a medical student and has continued ever since.

Finally, I am deeply thankful to my family and friends, who have always believed in me and supported me unconditionally. My greatest appreciation goes to my husband, who has been by my side since the moment I decided to become a doctor, providing endless support. I would also like to thank to my one-year-old son, who has accompanied me through the writing of this thesis — while the process might have been easier, it could never be happier.